International Journal of
*Plant Biology*

MDPI

*Article*

# Exploring the Role of Endophytes in *Cannabis sativa* L. Polyploidy and Agricultural Trait Improvement

**Ankita Srivastava [1], Timothy Sharbel [2] and Vladimir Vujanovic [1,*]**

[1] Department of Food and Bioproduct Sciences, University of Saskatchewan, 51 Campus Drive, Saskatoon, SK S7N 5A8, Canada
[2] Department of Plant Sciences, College of Agriculture and Bioresources, University of Saskatchewan, 51 Campus Drive, Saskatoon, SK S7N 5A8, Canada
* Correspondence: vladimir.vujanovic@usask.ca; Tel.: +1-306-222-7740

**Abstract:** Here, we examine the effects of ploidy variation in *Cannabis sativa* L. cell lines on the plant host genotype-associated microbiome. The endophytic microbiome has a protocooperative role in improving plant health and productivity and represents an alternative to synthetic chemical fertilizers and pesticides in sustainable agriculture. This study assessed the effects of seed endophytes on diploid and triploid Haze hemp cultivars. Key phenotypic characteristics were evaluated, revealing significant differences in seed germination in vitro as well as vegetative growth and flowering in phytotron conditions. Endophyte-treated triploid plants exhibited significantly taller heights compared to diploids ($p < 0.01$). These treated triploid plants also showed longer leaves at nodes 2, 6, and 8, except at node 4, indicating a plant in transition from vegetative growth to the generative developmental stage. Additionally, triploids treated with endophytes displayed the highest number of axillary branches, while endophyte-treated diploids had the fewest ($p < 0.05$). Both cultivars treated with endophytes exhibited a higher number of inflorescences compared to untreated control plants. This study revealed for the first time a direct correlation between the shifts in diameter of the stem and the biomass in both tested hemp hosts, in association with endophytic microbiomes.

**Keywords:** *Cannabis sativa* L.; microbiome; endophytes; diploid; triploid; microbial communities; axillary branches; inflorescences



**Citation:** Srivastava, A.; Sharbel, T.; Vujanovic, V. Exploring the Role of Endophytes in *Cannabis sativa* L. Polyploidy and Agricultural Trait Improvement. *Int. J. Plant Biol.* **2024**, *15*, 1118–1140. https://doi.org/10.3390/ijpb15040078

Academic Editor: Adriano Sofo

Received: 2 September 2024
Revised: 19 October 2024
Accepted: 24 October 2024
Published: 29 October 2024



## 1. Introduction

*Cannabis sativa* L. has been a part of human culture for centuries, evolving from Central Asia, and is primarily cultivated for food [1,2], seeds, fibers, textiles, bioenergy, recreation, and medicine [3–8]. Over the past 10 years, it has become increasingly popular in the biochemical and chemical industries due to the production of secondary metabolites, mainly $\Delta^9$ THC and CBD [9,10]. Although several types of beneficial microorganisms can be found in plants, the endophytes that reside inside the living cells of healthy host tissues play a significant role in providing resistance to biotic and abiotic stress [11]. In addition, they promote the growth, health, production, and biosynthesis of essential metabolites. Symbiosis between seed endophytes (SEns) and plants are ecologically important and globally prevalent associations [12–15], providing prenatal care to plants [16].

Hemp is a diploid species, and polyploid plants are now offered commercially, as polyploidy is a valuable tool in the genetic improvement of crop plants [17–20]. It provides various advantages, such as the increased vigor, size, and quality of leaves, flowers, and fruits [21,22]; improved tolerance to stress, pests, and diseases; the increased production of secondary metabolites, which can have medicinal or aromatic properties; protection from harmful mutations due to gene redundancy; and the ability to self-fertilize and overcome reproductive barriers [23–31]. Understanding the mechanism by which the microbiome acts in protocooperation [32,33] with ploidy in hemp is an important step towards microbiome-assisted agriculture and future hemp breeding programs.

The aim of this study is to assess the plant growth-promoting (PGP) potential of the seed microbiome associated with distinct *Cannabis sativa* ploidy level strains. Two sets of experiments were conducted. First, the *Cannabis sativa* T1 seed (2n) was randomly selected among non-commercial strains (https://www.blueskyhempventures.com (accessed on 1 April 2024) to evaluate the seed germination response in vitro in cocultures with a whole seed microbiome (WSM), seed endophytes (SEns), and epiphytes (SEps). Second, Suver Haze is the sativa commercial line used to evaluate the three microbial treatments on hemp genotype phenotypic responses and agriculture trait improvements under phytotron conditions, which are plant growth chambers. Suver Haze is the result of crossing a Neville's Haze male with a Krishna's Special female. Noteworthy for its high CBD content, mold resistance, and impressive yield, this strain is cherished for its calming effects. It is cultivated in both diploid (2n) and triploid (3n) lines, and these variations are typically 'seedless', as they do not tend to produce viable seeds [34–36]. In this study we hypothesized that the application of a native cannabis seed microbiome composed of WSM, SEns, and SEps communities on diploid and triploid hosts could induce an alteration in seed germination and exert distinct influences on plant growth promotion and phenotypic traits.

## 2. Materials and Methods

Two separate experiments were carried out on *Cannabis sativa* L. seeds to assess the effect of the seed microbiome composition on seed germination and agricultural plant host traits.

### *2.1. Cannabis Host Plants*

First, the whole seed microbiome of diploid (2n = 2x) *Cannabis sativa* T1 seed (https://www.blueskyhempventures.com (accessed on 1 April 2024)) and its influence on germinating hemp seeds in vitro was compared in separate treatments with seed epiphyte (SEp) and seed endophyte (SEn) inoculants. Second, we used the purchased (GTR, Independence, OR, USA) diploid (2n = 2x) and triploid (2n = 3x) lines of Suver Haze (sativa) and evaluated WSM, SEn, and SEp microbial treatments on seed germination and various agricultural traits under phytotron conditions.

A phylogenetic assessment of the *C. sativa* T1 line was determined by DNA sequencing of the MADC6, a sex-related gene. SCAR primers (sequence-characterized amplified region): SCAR119_F (5′-TCA AAC AAC AAA CCG-3′) and SCAR_119_R (5′-GAG GCC GAT AAT TGA CTG-3) [37] were also used as they are the most reliable for evolutionary analysis [38]. An evolutionary tree was rooted with *Vitis vinifera*, often used as a model plant for rRNA sequence analyses and floral development [39], and was inferred by using the maximum likelihood method with 1000 bootstrap and the Tamura–Nei model [40]. The tree with the highest log likelihood (−9416.12) is shown. Initial tree(s) for the heuristic search were obtained automatically by applying neighbor-join and BioNJ algorithms to a matrix of pairwise distances estimated using the Tamura–Nei model, and then selecting the topology with the superior log likelihood value. The tree was drawn to scale, with branch lengths measured in the number of substitutions per site. This analysis involved 6 nucleotide sequences. There was a total of 3475 positions in the final dataset. Evolutionary analyses were conducted in MEGA11 [41].

### *2.2. Inoculum Preparation*

Visually healthy cannabis seeds were packed in aluminum foil sealed bags and kept at 4 °C for long term storage [42]. Seeds were rinsed in 95% ethanol for 10 s prior to sowing on potato dextrose agar (PDA) plates without antibiotics; the plates were incubated at 23 °C in darkness to allow germination until 1 cm radicle emergence [43,44]. There were three seed microbial communities that were reintroduced to seeds as inoculants: seed epiphytes (SEps from outer seed part or coat), seed endophytes (SEns from inner seed part comprising endosperm and embryo), and the whole seed microbiome ((WSM) from both outer and

inner seed parts), respectively. There was a negative control in which only seeds were grown without any treatments. All seeds were properly sterilized (Figure 1).

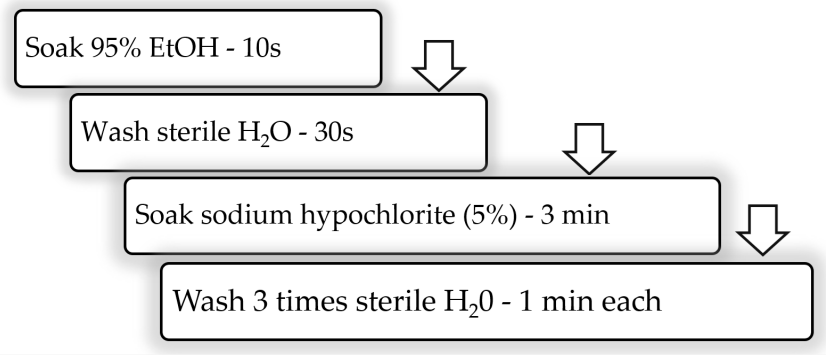


**Figure 1.** Surface sterilization procedure for seeds.

For the whole seed WSM inoculum preparation, 5 seeds were used to prepare a stock of the inoculum. A pestle and mortar were employed for crushing and grinding them into a powder to be submerged in 900 µL of sterile distilled water to obtain a fine paste as an initial stock. A total of 100 µL of the sample was taken from the initial stock for serial dilutions to obtain $2 \times 10^4$ cells/mL inoculum. A total of 200 µL of $2 \times 10^4$ cells/mL were placed at the center of the petri plate [45,46] as a seed inoculation method (Figure 2). For seed endophytes (SEns), seed coats were removed from 5 seeds and then germinated until 1 cm of the radicle was visible. Germinants were crushed with pestle and mortar in the presence of 900 µL of sterile distilled water. For seed epiphytes (SEps), 5 cannabis seed coats were removed and crushed with the same quantity as mentioned above with pestle and mortar. The same dilutions were prepared and used for all 3 treatment studies (Figure 2).

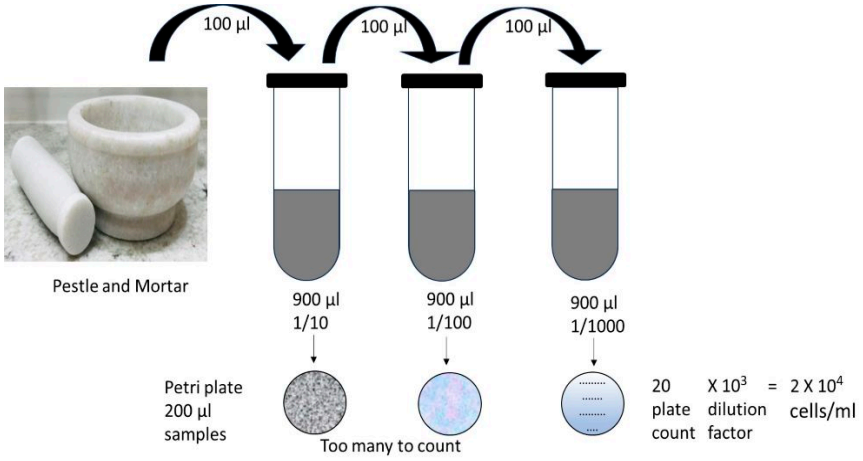


**Figure 2.** Serial dilutions of seed endophytes (SEns) prepared to $2 \times 10^4$ cells/mL.

Peat, sand, and vermiculite were prepared in the ratio of 3:2:1 and added to a sterile petri plate. Five fresh hemp seeds (https://www.blueskyhempventures.com (accessed on 1 April 2024)) were allowed to germinate at equal distances from each other in a circle in 1 petri plate after proper sterilization. After the 2nd day of germination, 200 µL of the WSM, SEn, and SEp inoculum preparation were added individually to the centers of different petri plates [45] (Figure 3).

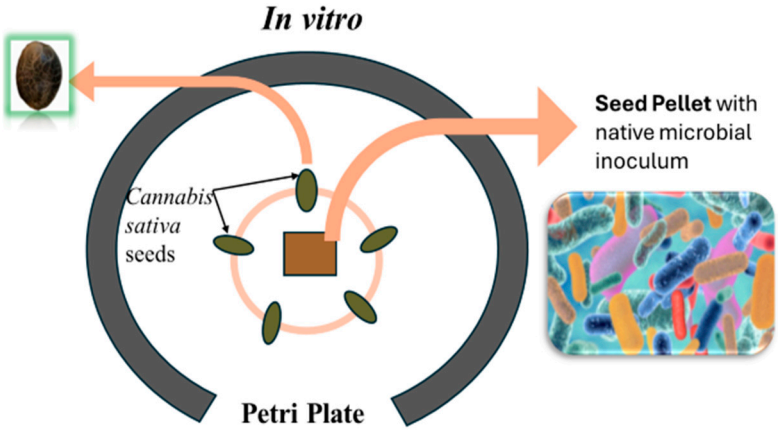


**Figure 3.** In vitro method used for reintroducing a native seed microbiome on germinating *Cannabis sativa* seeds [45]. Microbial inoculum consisted of ground *Cannabis sativa* seeds prepared as a pellet, containing seed microbiome embedded in embryonic and endospermic healthy tissue/cells as a suitable substrate or medium to fortify seed recolonization by microbes (see for detail in M & M).

### *2.3. Experiment 1—In Vitro*

#### 2.3.1. Seed Germination Assay

Cannabis T1 line seeds were germinated in 100 mm × 15 mm petri plates, and the germination rate was calculated at days 2, 4, 7, and 10 of each treatment for SEps, SEns, and WSM, including seeds without any treatment as a control [47]. Five seeds were plated in triplicate on PDA and kept in dark at a room temperature of 21 °C (Figure 3). When radicles of 1 cm in length came out, the inoculum pellet, a powder of seeds containing native microbiome, was added to the center of the 10 cm petri dish. The mean and standard error were determined for various experiments, including seed germination, weight of the germinant, and radicle size.

#### 2.3.2. Identification of Fungal and Bacterial Taxa

Seeds, flowers, and leaves from both diploid and triploid Suver Haze plants were allowed to grow on separate potato dextrose agar (PDA) for a week and pure cultures were obtained by transferring the individual colony type from mixed cultures to the fresh agar plate. Colony forming units were calculated for each pure culture obtained and their morphology was identified and validated based on DNA sequences [44]. Genomic DNA from these pure cultures were extracted using DNeasy Plant Kit # 69104 (Company—Qiagen, Toronto, ON, Canada), which were then amplified using forward (CS1_ITS3_KYO2-5′-ACA CTG ACG ACA TGG TTC TAC AGA TGA AGA ACG YAG TRAA-3′) and reverse (CS2_ITS4-5′-TAC GGT AGC AGA GAC TTG GTC TTC CTC CGC TTA TTG ATA TGC-3′) universal ITS primers [48,49]. PCRs were performed in a reaction volume of 25 µL consisting of 10 ng/µL DNA, 1× buffer with 2 mM $MgCl_2$ 0.2 mM dNTPs, 0.5 µM forward and reverse primers, and 0.1 U Taq polymerase. Amplifications were performed for initial denaturation at 95 °C for 5 min, followed by 40 cycles of denaturation at 95 °C for 30 s annealing at 58 °C for 45 s and extension at 72 °C for 45 s with completion at the final extension of 72 °C for 5 min. A PCR product of 400 bp was run on 1.2% agarose gel made in 0.5× TAE buffer, and then gel extraction was performed with Qiagen gel extraction kit Catalog # 28704, which was then sent for sequence analysis by the Sanger method to the NRC (National Research Council, Saskatoon, SK, Canada).

The same parts of the plants were also grown on Luria–Bertani (LB) plates for bacterial isolation and incubated at 21 °C over 3 days. The dilution series was applied [50] to isolate bacteria and purified colonies from mixed bacterial cultures. Genomic DNA from each purified culture were extracted using DNeasy Plant Kit # 69104 (Company—Qiagen), which were then amplified using forward (CS1_341-5′-ACA CTG ACG ACA TGG TTC TAC ACC TAC GGG NGG CWG CAG-3′) and reverse (CS2_806-5′-TAC GGT AGC AGA GAC TTG

GTC TGA CTA CHV GGG TAT CTA ATC C-3′) universal 16S rRNA primers [51]. PCRs were performed in a reaction volume of 25 µL consisting of 10 ng/µL DNA, 1× buffer with 2 mM $MgCl_2$, 0.2 mM dNTPs, 0.5 µM forward and reverse primers, and 0.1 U Taq polymerase. Amplifications were performed for initial denaturation at 95 °C for 5 min, followed by 40 cycles of denaturation at 95 °C for 30 s annealing at 60 °C for 45 s and extension at 72 °C for 45 s, with completion at the final extension of 72 °C for 5 min. PCR products of 450 bp were run on 1.2% agarose gel made in 0.5× TAE buffer, and then gel extraction was performed with Qiagen gel extraction kit Catalog # 28704, which was then sent for sequence analysis by the Sanger method to the NRC (National Research Council, Saskatoon, SK, CanadaSaskatoon. Relative abundance of fungal and bacterial communities was calculated by counting the number of colonies found on the PDA and LB plate; its frequency by richness and evenness was calculated using the Shannon–Weiner diversity index.

### *2.4. Experiment 2—In Phytotron*

The most effective seed endophytic (SEn) microbiome tested under Experiment 1 was applied on diploid and triploid Suver Haze, commercial cultivars of *C. sativa* plants, as presented in Figure 3. The germinants were grown in vitro for 5 days under laboratory conditions and were transferred from petri dishes to separate plastic trays (filled with sterilized peat, sand, and vermiculite; ratio 3:2:1) to avoid cross-contamination between treatments. Roots were covered with 0.6 cm of sterile Sunshine 4 soil and seedlings were watered regularly. After 1 week of growth and adaptation, the seedlings were transplanted into large 4 L pots with Sunshine 4 soil for growing in Phytotron chambers. The phytotron conditions were controlled on a daily basis to maintain light (16:8 h of light/dark using T5HO835 Fluorescent lamps at 3500 K color temp), temperature (25 °C), and humidity (55–60%). During the flowering phase of the plant, the light was switched to a 12:12 h, light/dark regime. All experiments were performed in triplicate; data were collected and statistically analyzed.

#### Plant Phenotypic Traits

Plant height was measured using a ruler on three randomly selected replicates every week for 10 weeks. The length and width of the leaves were also measured on 3 randomly selected replicates at nodes 2, 4, 6, and 8. Measurements of nodes 2, 4, 6, and 8 were obtained at weeks 2, 5, 7, and 10, respectively.

The days of flowering and senescence were evaluated by assessing the number of days before plant flowering, maturation, and senescence. The estimated marginal means of days of flowering and senescence were calculated on three randomly selected replicates. Also, the estimated means of the number of axillary branches (n = 3; taken every week when flowering started until plant reached senescence), the number of inflorescences assessed in mature flowering plants, and the internodal distances, were also monitored every week when flowering started and reached senescence [52–54].

When plants reached senescence, fresh shoot weights were measured for randomly selected plants (n = 3) and then those plants were kept in a desiccator for 3–4 days until shoots were dried. Comparisons were made for fresh and dry plant samples [47,55].

Measurement of photosynthesis by a chlorophyll fluorometer is a common method used to assess the health of every crop plant, including hemp [56,57]. It involves measuring the maximum efficiency of photosystem II (PSII) photochemistry in dark-adapted leaves. To determine this ratio, a weak modulated measuring beam is applied to determine the minimal fluorescence yield in a dark-adapted leaf (F0), and a saturating flash is then superimposed to induce the maximal yield of chlorophyll fluorescence (Fm) [58,59]. An Fv/Fm value in the range of 0.79 to 0.84 is considered optimal for many plant species, with lower or higher values indicating plant physiological stress (3 replicates of each treatment were used).

Transparent tape was used as a traditional method to measure stomatal size (SS) and density (SD); stomata cover the epidermis of leaves and play an important role in physiological behavior of plants [60,61]. The tape allowed for making the impression and viewing stomata under a microscope for completing the analyses [62].

### *2.5. Statistics and Principal Component Analysis*

Statistical analyses for all the above parameters were performed using a one-way analysis of variance (ANOVA) technique, which was followed by post hoc Tukey's honest significant difference (HSD) and least significant difference (LSD) tests to determine the statistical significance at $p \leq 0.05$ using SPSS (IBM SPSS statistic 22).

Principal component analysis (PCA) was used as a dimensionality reduction technique to analyze patterns in multivariate experimental data [63,64]. A Bray–Curtis dissimilarity matrix was calculated between all pairs of samples based on the relative abundances of different parameters considered here using Origin Pro 8 software [65]. The dissimilarity matrix represents the pairwise differences in composition between samples.

Principal component analysis (PCA) is an effective approach to measure genetic divergence between germplasm genotypes with respect to their characteristics. The PCA graphical presentation was generated by using Origin Pro 8 software. In this software, data were normalized using Min-Max Scaling where scaling data were selected accordingly. Ten parameters were selected for all four different cultivars with 6 samples in each parameter for the analysis [66,67].

## 3. Results

### *3.1. Experiment 1*

#### 3.1.1. *Cannabis sativa* T1 Strain

To assess the identification of the *Cannabis sativa* T1 strain (GenBank accession no. PQ479350;), a phylogenetic tree rooted with *Vitis vinifera* was created using the MADC6 sexual gene (Figure 4). The T1-MADC6 sequence blast against the GenBank public database (https://www.ncbi.nlm.nih.gov/genbank/ (accessed on 1 April 2024)) resulted in 97% similarity with *C. sativa* GenBank accession no. AF364955. The results of evolutionary phylogenetic analyses based on the maximum likelihood method showed that the T1 strain forms a unique clade with typical *C. sativa* strains closely related with its marker gene deposited in GenBank (AF364955).

#### 3.1.2. Dynamic of T1 Germination

The highest percentage of seed germination was recorded on day 4, while the lowest was seen on day 2 in all treatments (Figure 5). Untreated seeds (control) show a pronounced germination at day 2 and day 4, while germination for the whole seed microbiome (WSM), epiphyte (SEp), and endophyte (SEn) treatments shifted with a peak on day 7 and 10 when compared to the control group.

The cumulative germination over 10 days of incubation (Figure 6) shows that the whole seed (WS) microbiome was correlated with the highest percentage of germination as compared with the individually applied functional group of epiphytes (SEps) and a similar percentage of germination with endophytes (SEns).

#### 3.1.3. Germinant Biomass Formation and Radicle Size

Germinative biomass was measured on day 5 (Figure 7) during the phase of maximum germination rate (Figure 5). By day 5, the lowest germinant biomass was produced under the control and WS microbiome treatments, an increased biomass was produced under SEp treatment, and maximum biomass was induced by the SEn treatment (Figure 7A). Similarly, the radicle size (Figure 7B) was more pronounced under SEn compared to the SEp and WSE treatments.

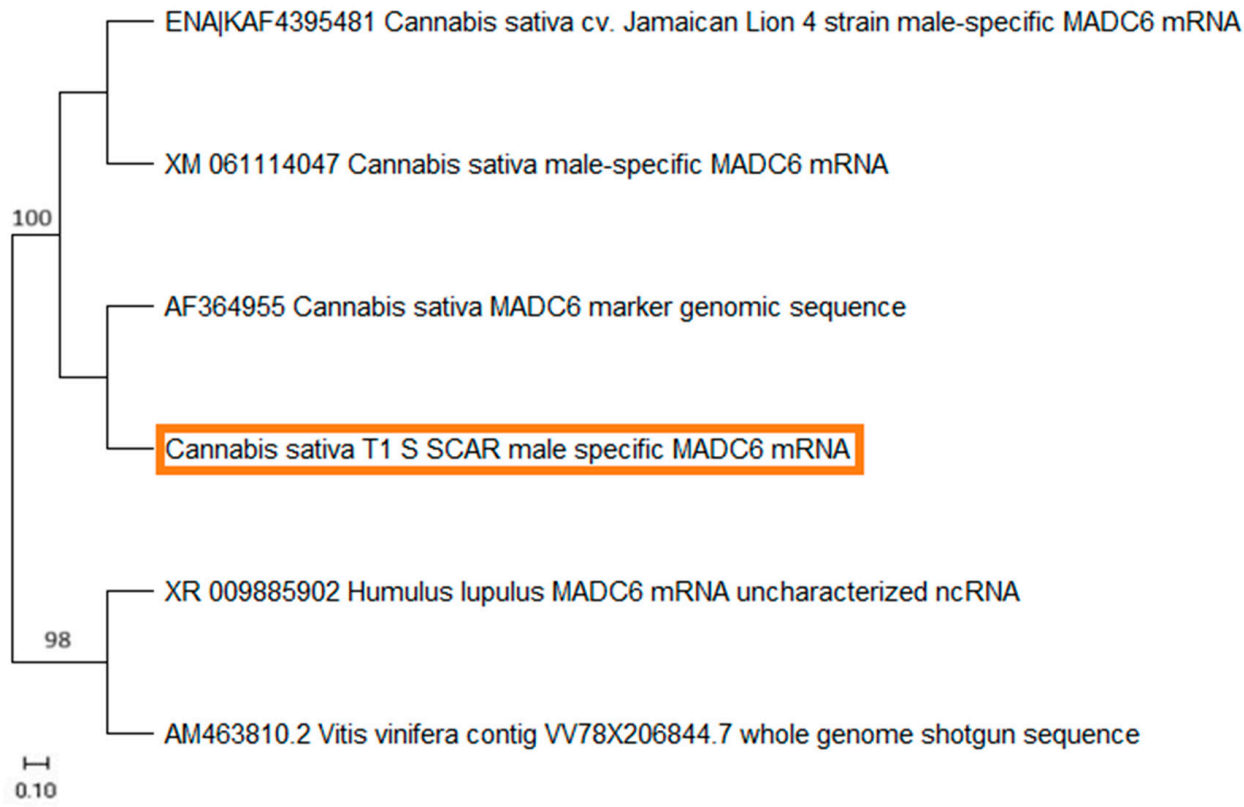


**Figure 4.** Male-specific MADC6 evolutionary position of *Cannabis sativa* T1 strain (GenBank accession no. PQ479350) using maximum likelihood method with 1000 bootstrap. Numbers above the nodes are bootstrap values. The tree is rooted with *Vitis vinifera* (Gene Bank accession no. AM463810.2). The red box indicates the phylogenetic position of the T1 strain.

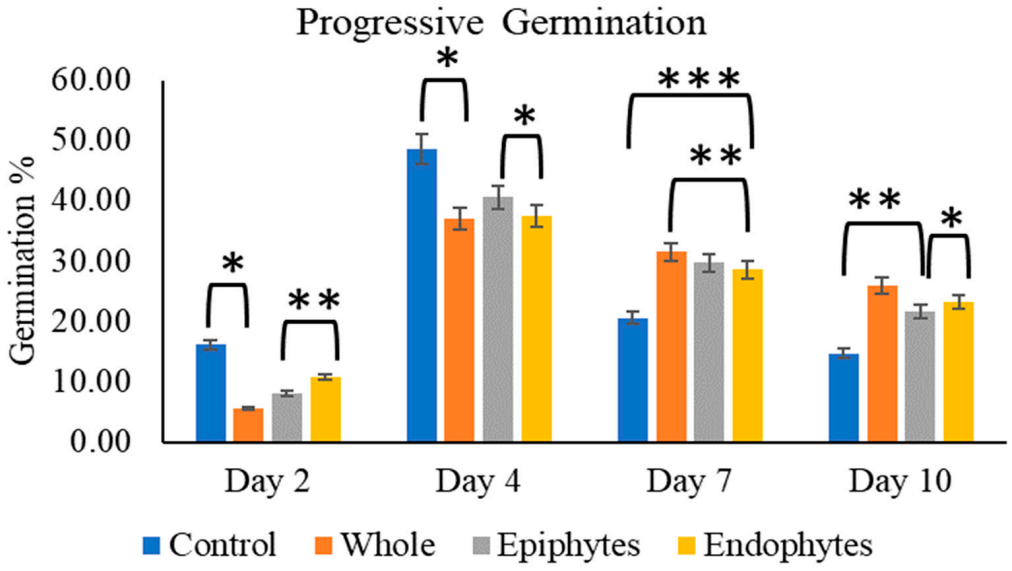


**Figure 5.** Progressive germination of *Cannabis sativa* seeds T1 on days 2, 4, 7, and 10 under different treatments of seed epiphytes (grey), seed endophytes (yellow), and whole seed microbiome (orange). Data are means and standard errors of three replicates (two-way ANOVA with LSD test, * $p < 0.05$, ** $p < 0.01$, *** $p < 0.001$).

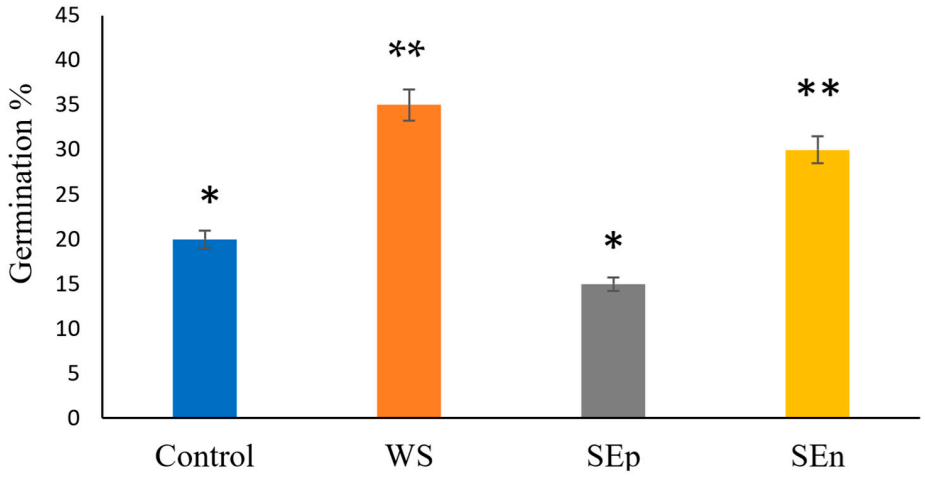


**Figure 6.** Cumulative germination percentage of *Cannabis sativa* seeds T1 treated with whole seed microbiome (orange), seed epiphytes (grey), seed endophytes (yellow), and control—without treatment (blue). Data are means and standard errors of three replicates (one-way ANOVA, * $p < 0.05$, ** $p < 0.01$). WS—whole seed, SEp—seed epiphyte, and SEn—seed endophyte.

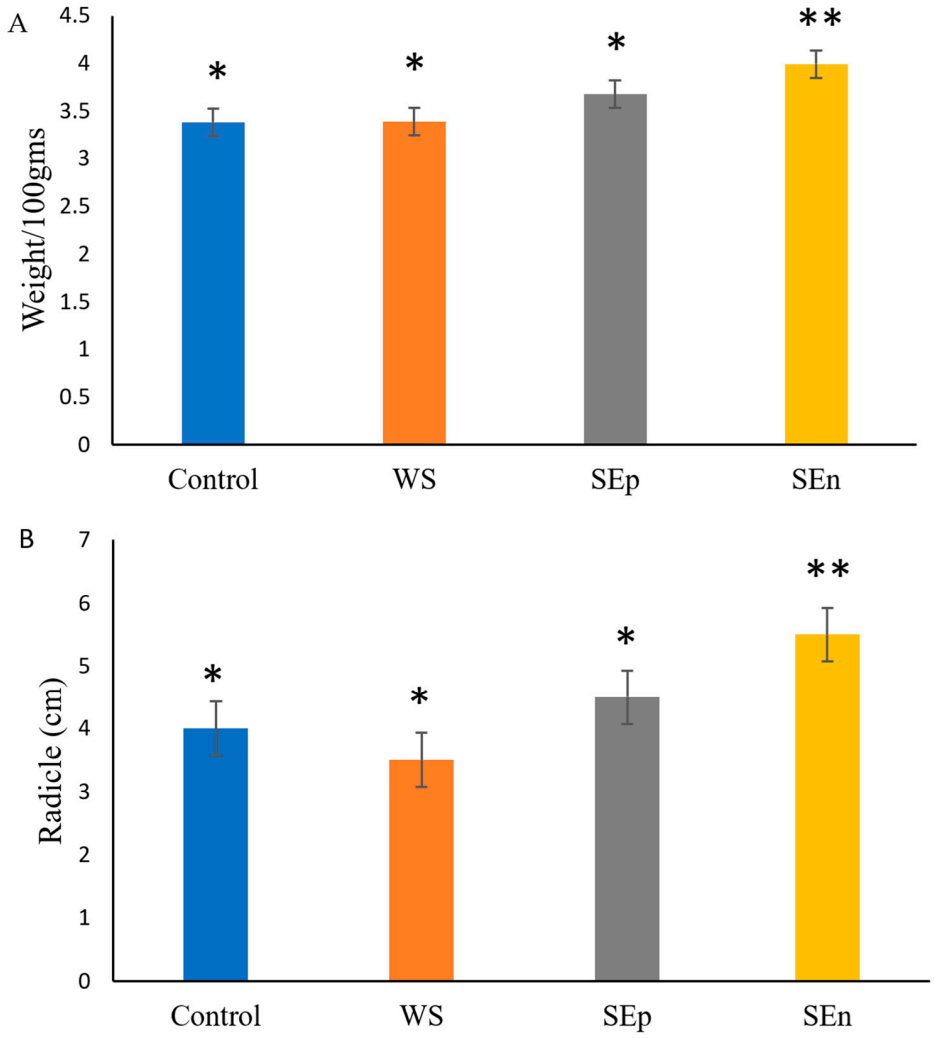


**Figure 7.** Dynamic of *Cannabis sativa* T1 seed germination displays germinant biomass formation (**A**) and size of the radicle (**B**) on day 5. Data are means and standard errors of three replicates (one-way ANOVA, * $p < 0.05$, ** $p < 0.01$). WS—whole seed, SEp—seed epiphyte, and SEn—seed endophyte.

### *3.2. Experiment 2*

#### 3.2.1. Diversity of Fungi and Bacteria

The microbial communities of cannabis plants treated with the same SEn seed microbiome showed important host genotype-dependent structural differences. The culturable endophytic microbiome of the diploid Suver Haze cultivar was composed of 46 fungal (ITS rRNA) and 62 bacterial (16S rRNA) strains. The triploid Suver Haze showed a decreased number of both fungal and bacterial inhabitants, with 24 and 28 strains, respectively. In terms of the fungal community composition (Figure 8), *Penicillium*, *Fusarium*, and *Cladosporium* genera dominated in diploid cultivars, whereas *Penicillium* and *Chaetomium* were dominant in triploid cultivars, with *Alternaria* strains as codominant. While *Penicillium* and *Alternaria* mainly occupied seeds, *Penicillium*, *Fusarium*, *Alternaria*, and *Chaetomium* colonized flowers. *Aspergilus* was only detected in triploid host leaves. In terms of the relative bacterial diversity (Figure 9), *Bacillus*, *Streptomyces*, and *Klebsiella* were the dominant genera in diploid cultivars. In particular, *Bacillus* showed very high—an 85% abundance—in the triploid Suver Haze host. While *Bacillus* occupied all diploid and triploid hosts organs, *Streptomyces* mainly occurred in flowers, while Enterobacteria (*Enterobacter*, *Pantoea*, *Klebsiella*, and *Erwinia*) dominated in leaves.

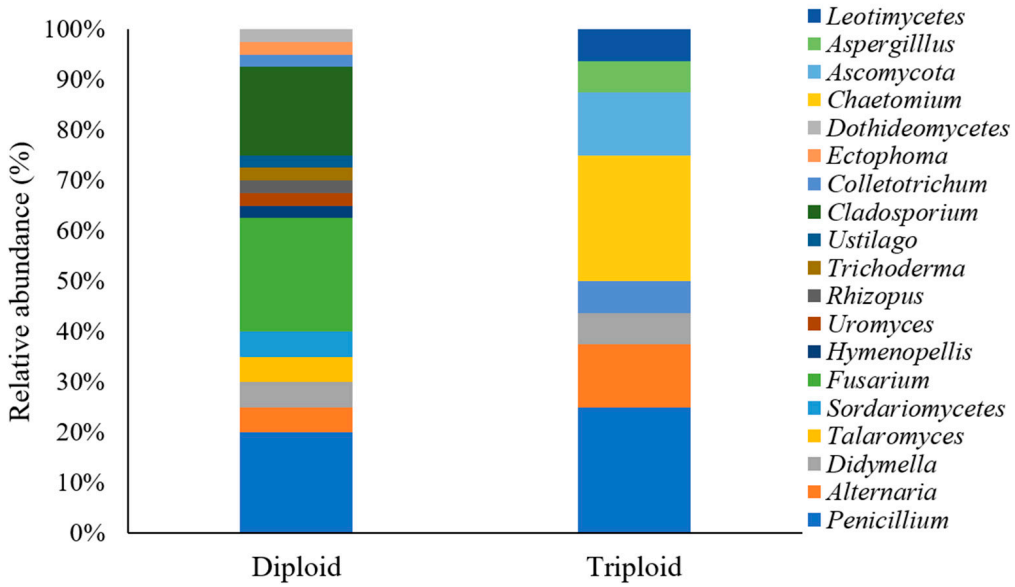


**Figure 8.** Relative abundance of fungal taxa in diploid and triploid plant hosts. The unknown genera of fungi were regrouped within the taxonomical orders. (Shannon–Weiner diversity index calculated for diploid H = 2.29 and triploid H = 1.9).

#### 3.2.2. Plant Growth Dynamics

The untreated diploid Suver Haze plants were taller than seed endophyte (SEn) treated diploid plants. The results were persistent over time or between 3 and 10 wks of assessment (Figure 10A). The opposite characteristics were observed in the triploid host (Figure 10B), where untreated triploid plants (control) were shorter as compared to SEn treated plants. In addition, the average triploid plants were taller (~120) cm than diploid (~90–100 cm) plants.

#### 3.2.3. Leaf Size and Nodes

The length (Figure 11) and width (Figure 12) of leaves were measured in diploid and triploid Suver Haze genotypes on nodes 2, 4, 6, and 8. It was found that node 2 of the untreated diploid plant showed an increased length of leaves as compared to the SEn-treated plant, whereas at nodes 4, 6, and 8, SEn-treated diploid plants have increased length compared to the untreated control. In the case of triploids, at nodes 2, 6, and 8, seed

endophyte-treated plants showed increased length as compared to the untreated plant; however, at node 4, it was exactly the opposite. Overall, the triploid plants showed longer leaves (~15 cm) compared with diploids (~10 cm). In diploid plants treated with seed endophytes, leaf width was greater compared to untreated diploid plants. Conversely, in triploid plants at the 4th, 6th, and 8th nodes, untreated triploid leaves exhibited a broader size in comparison to seed endophyte-treated triploids. The opposite was recorded for the second node.

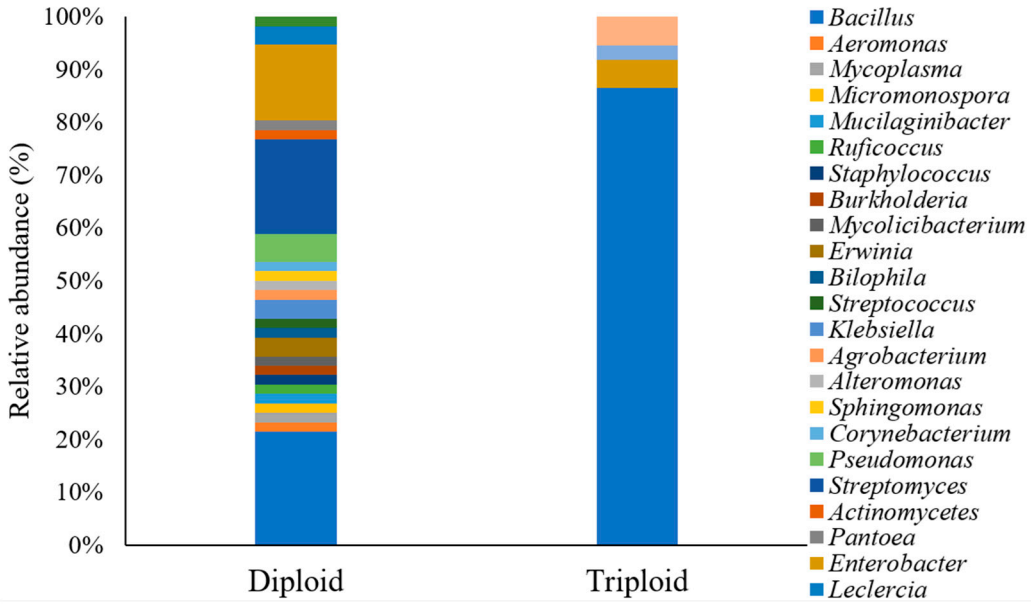


**Figure 9.** The relative abundance of bacterial taxa in diploid and triploid plant hosts. The unknown genera of bacteria were regrouped within the taxonomical orders. (Shannon–Weiner diversity index calculated in diploid H = 2.65 and triploid H = 0.53).

### 3.2.4. Timelines of Flowering and Senescence

A negative disparity in flowering durations (Figure 13A) between control (~100 days) and seed endophyte-treated diploid plants (~96 days) was found; however, in triploids, the endophyte-treated plants showed reduced flowering time (~85 days) when compared to their untreated counterparts (~100 days). The days of senescence (Figure 13B) were increased in seed endophyte-treated diploids (~155 days) and triploids (~180 days) as compared to their control counterparts (~150 days). Overall, both diploid and triploid plants treated with seed endophytes experienced longer growth phases as compared to untreated ones.

### 3.2.5. Quantitative Analysis of Branching Architecture

The number of axillary branches (Figure 14A) was the highest in triploids treated with SEn and lowest in diploids treated with SEn compared to the untreated control (A). The number of inflorescences (Figure 14B) was higher in SEn-treated diploids (~105) and triploids (~118) as compared to their non-treated counterparts (~90). A greater number of inflorescences was directly proportional to more flowers (Figure 14B). Figure 14C showed that the internodal distance is highest in the SEn-treated triploid plants (7.5 cm) and lowest in the SEn-treated diploid plants (5 cm), indicating that the values in untreated plants in both hemp genotypes lie in between these ranges.

### 3.2.6. Correlation Between Photosynthetic Rates and Stomatal Impressions

Figure 15A showed the photosynthesis (PSII) Fv/Fm ratio which was in the range of 0.79–0.83. The high number of stoma imprints was found in triploid (~170) as compared to diploid (~150) plants (Figure 15B).

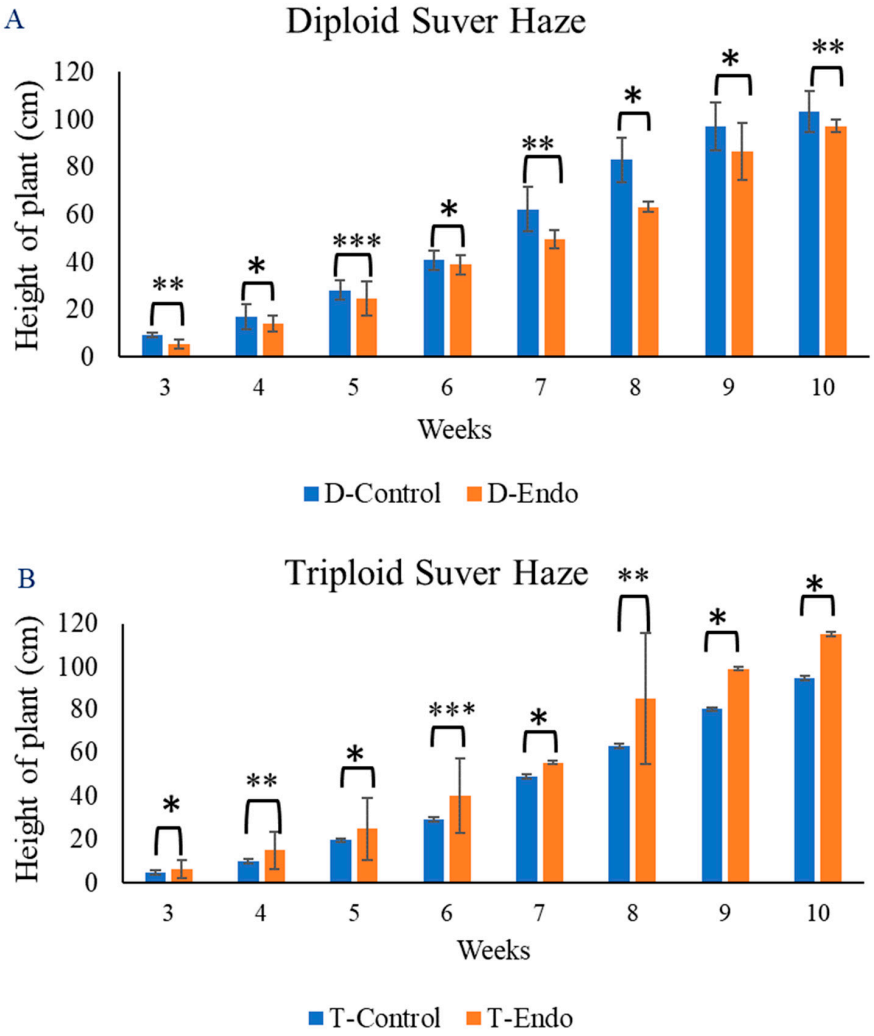


**Figure 10.** Plant height growth dynamics measured at different node stages in Suver Haze diploid (**A**) and triploid (**B**) plants. Measurements were obtained at weeks 3, 4, 5, 6, 7, 8, 9, and 10. D-Control: diploid control; D-Endo: diploid SEn; T-Control: triploid control; T-Endo: triploid SEn. Data are means and standard errors of three replicates (two-way ANOVA with LSD test, * $p < 0.05$, ** $p < 0.01$, *** $p < 0.001$).

### 3.2.7. Shoot and Root Biomass

It was observed that fresh shoot weight increased in seed endophyte-treated triploid plants (~65 g), whereas it was the lowest in SEn-treated diploid plants (~50 g). In terms of the dry shoot weight, the highest values were recorded in untreated diploid plants (~25 g) and the lowest in untreated triploid cultivars (~15 g). A linear regression analysis of diploid and triploid plants (Figure 16A,B) showed the effect of fresh and dry shoot weight compared with the diameter of the stem ($R^2$ = 0.93–0.98). As the diameter of the stem increases, so does the biomass of the shoots. Slope rate was increased in diploids as compared with triploids and a greater rate of change in fresh shoot and dry shoot in diploids were seen compared with triploids. The slope angle in the diploid fresh shoot and triploid fresh shoot was found to be 13° and 9°, respectively, whereas it was 7° and 4° in the dry shoot diploids and triploids, respectively. Further, the analyses showed the fresh (Figure 17A) and dry root (Figure 17B) weight compared with the diameter of the stem ($R^2$ = 0.89–0.96). The fresh root weight was the highest and the same in seed endophyte-treated and untreated triploid cultivars (~15 g), whereas it was the lowest in seed endophyte-treated diploid cultivars (~7 g). Regarding dry root weight, it was increased from the diploid untreated (~1.8 g) to the SEn-treated diploid (2.75 g), being the highest in untreated triploid (3.1 g) plants with a slight decrease in SEn-

treated triploids (2.5 g). A linear regression analysis of diploid and triploid plants in Figure 17 showed that the rate of change in fresh root diploids and triploids was greater than in dry root diploids and triploids. The weight of the root in diploids ranged from 7 to 12 g whereas in triploids, it ranged from 12 to 18 g. The slope angle for diploid fresh roots and triploid fresh roots was consistent at 10°, indicating a similarity in their profiles. In contrast, both diploid and triploid dry shoots exhibited a slope angle of 4°.

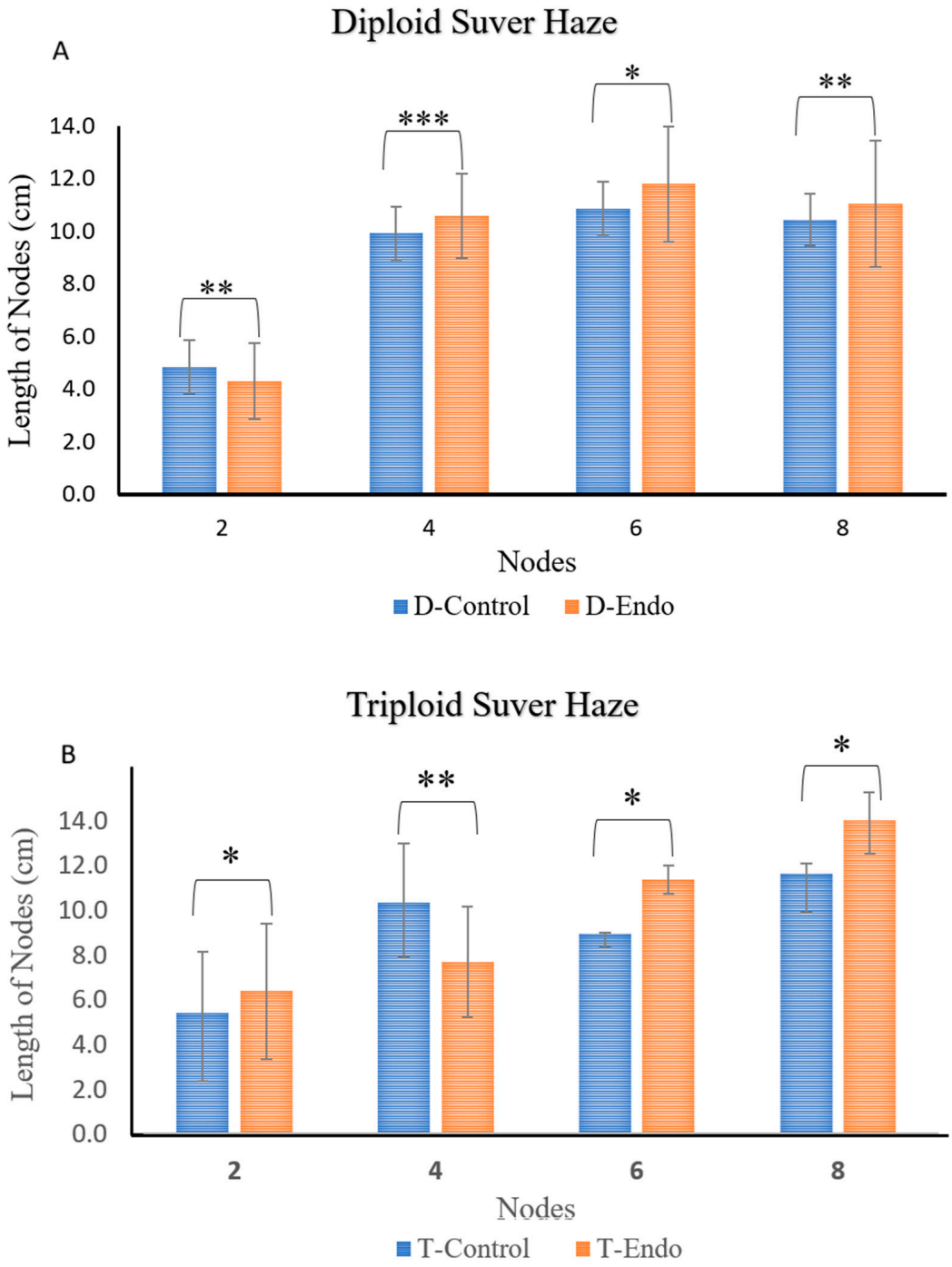


**Figure 11.** Length of leaves at different nodes in diploid (**A**) and triploid (**B**) plants during the vegetative phase of the Suver Haze life cycle. Measurements were obtained at weeks 2, 5, 7, and 10 for nodes 2, 4, 6, and 8. D-C-diploid control; D-Endo-diploid SEn; T-C-triploid control; T-Endo-triploid SEn. Data are means and standard errors of three replicates (two-way ANOVA with LSD test, * $p < 0.05$, ** $p < 0.01$, *** $p < 0.001$).

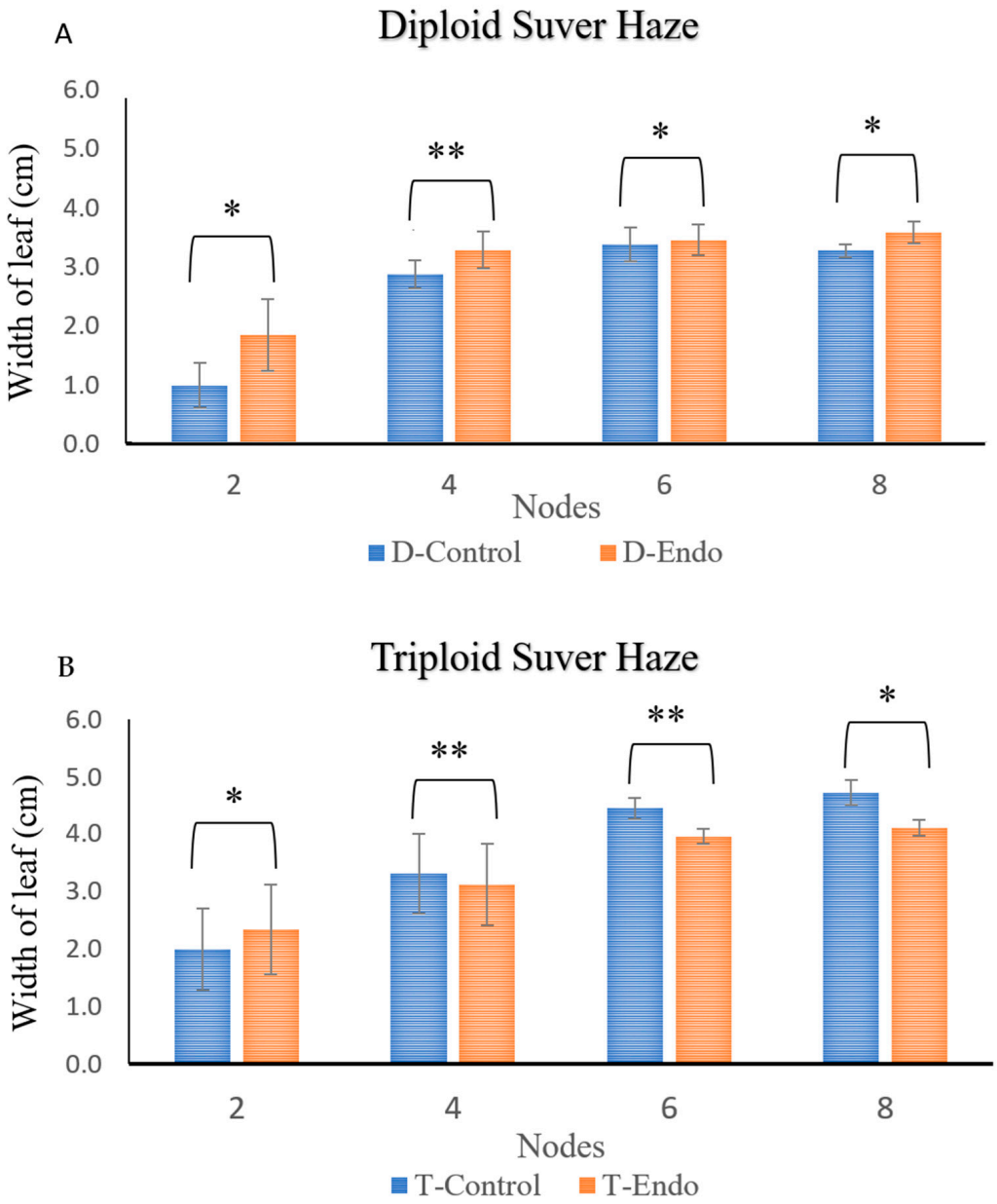


**Figure 12.** The width of leaves at different nodes in diploid (**A**) and triploid (**B**) plants during the vegetative phase of the Suver Haze life cycle. Measurements were obtained at weeks 2, 5, 7, and 10 for nodes 2, 4, 6, and 8. D-C: diploid control; D-Endo: diploid SEn; T-C: triploid control; T-Endo: triploid SEn. Data are means and standard errors of three replicates (two-way ANOVA with LSD test, * $p < 0.05$, ** $p < 0.01$).

### 3.2.8. Principal Component Analysis—Hosts, Traits, and Treatments

Principal component analysis (PCA) calculated using Bray–Curtis measurements (Figure 18) showed that the length of leaves was clustered with the untreated diploid between the PC2 axis on the positive side and PC1 on the negative side. In the opposite direction, the width of leaves and PstII (photosynthesis) were clustered till the positive side of the PC1 axis and the negative side of the PC2 axis; this cluster seems to not be specifically associated to any cultivar or treatment tested. The flowering days and phytohormone levels clustered together in both the diploid and triploid untreated cultivars. This clustered till the negative side of both the PC1 and PC2 axes. Further, the phytocannabinoid, inflorescence, senescence, height, and internodal distances are closely related to triploid endophytes as a separate cluster between 61.46% and 29.76% of the total variance, respectively.

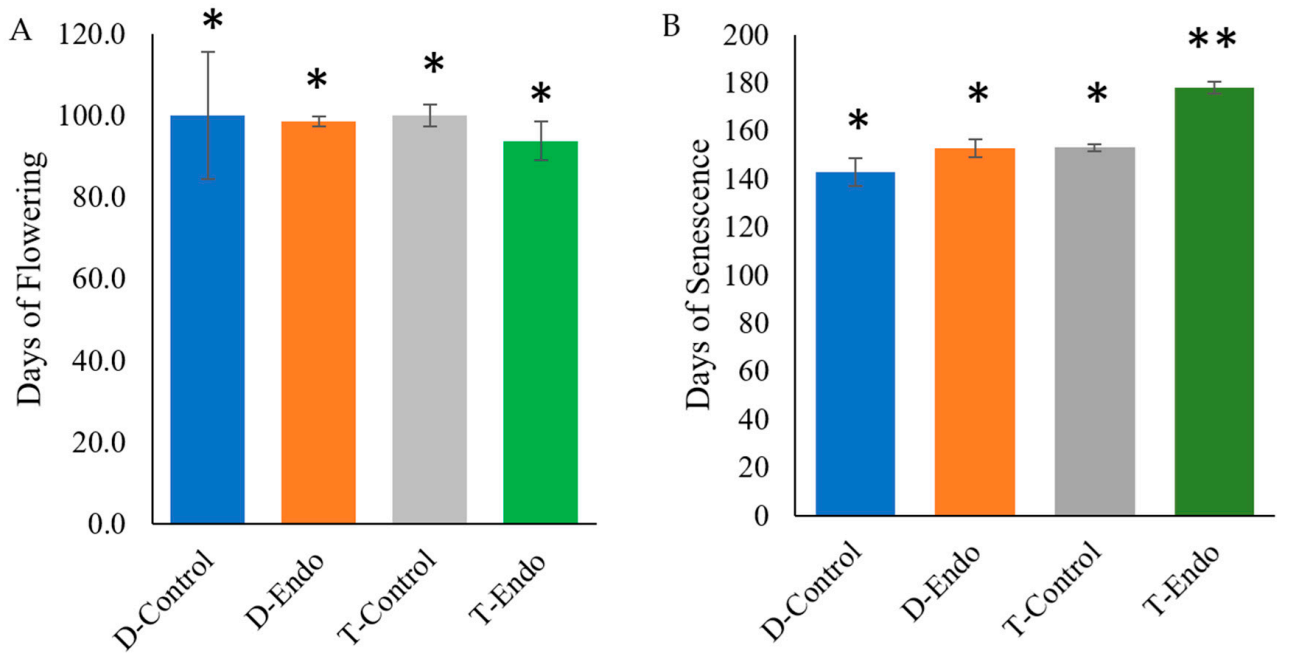


**Figure 13.** Days of flowering (**A**) and senescence (**B**) were calculated for different treatments in Suver Haze plants. D-Control: diploid control (blue); D-Endo: diploid SEn (orange); T-Control: triploid control (grey); T-Endo: triploid SEn (green). Data are means and standard errors of three replicates (one-way ANOVA, * $p < 0.05$; ** $p < 0.01$).

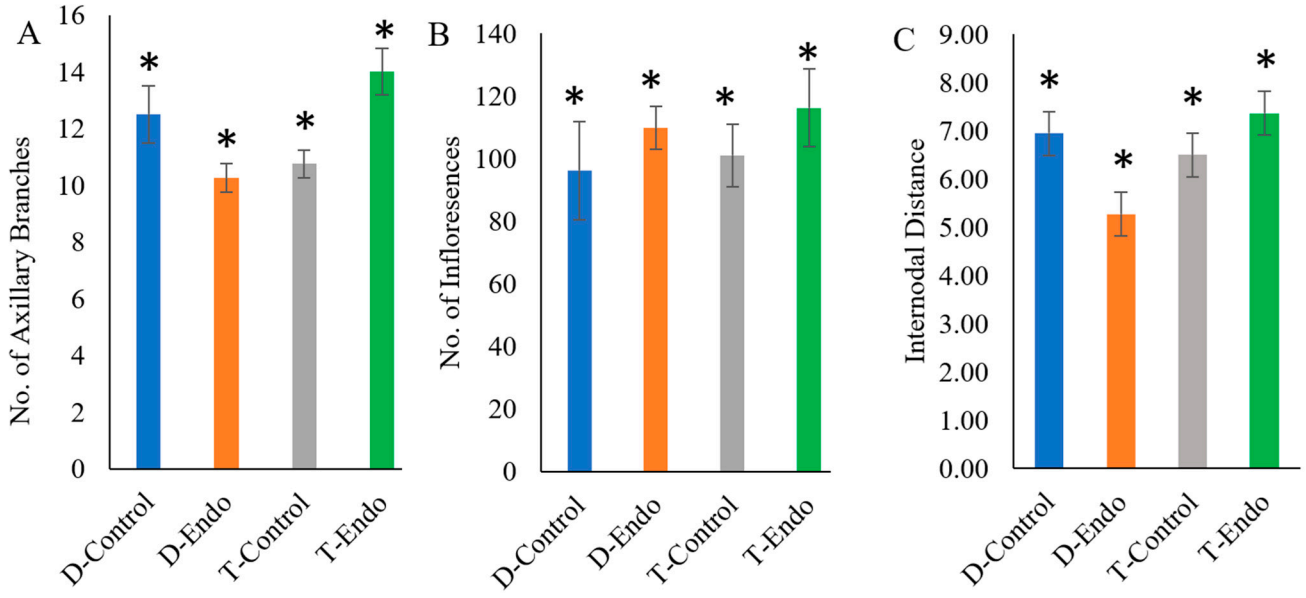


**Figure 14.** Number of axillary branches (**A**), inflorescence (**B**), and means of internodal distance (**C**) calculated for different treatments of Suver Haze plants. D-Control: diploid control (blue); D-Endo: diploid SEn (orange); T-Control: triploid control (grey); T-Endo: triploid SEn (green). Data are means and standard errors of three replicates (two-way ANOVA, * $p < 0.05$).

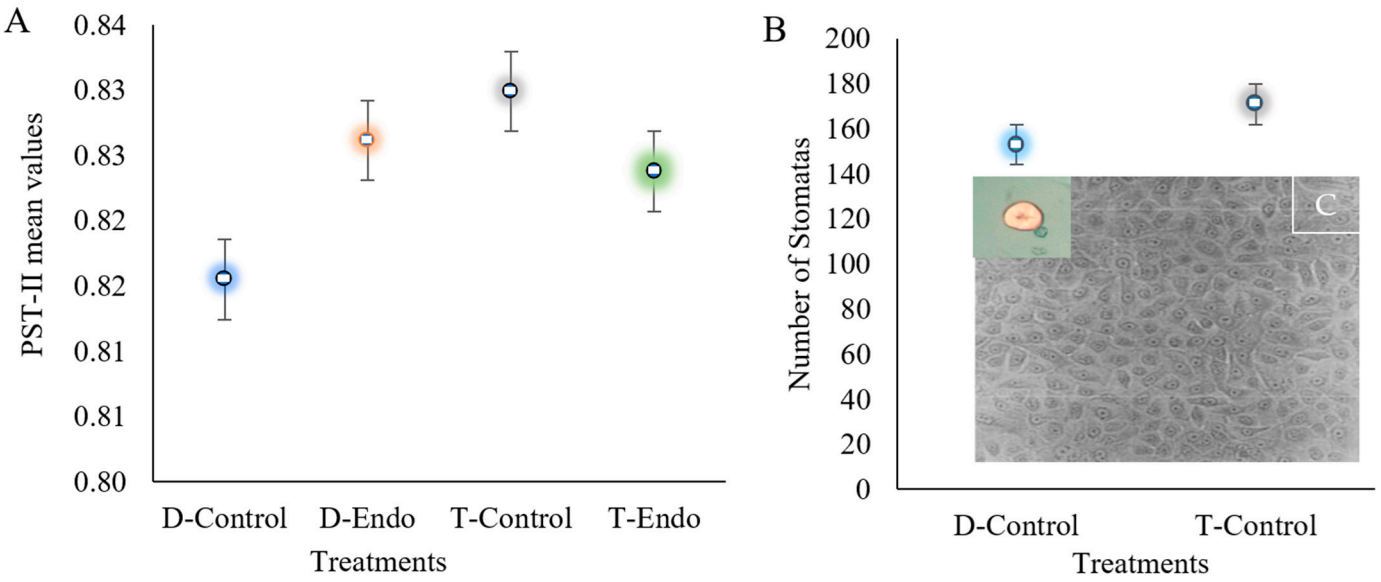


**Figure 15.** (**A**) Fv/Fm ratio calculated for different treatments on 2 lines of Suver Haze hemp cultivar; (**B**) represents the number of stomata present on diploid and triploid plants. Photomicrograph of the abaxial leaf surface taken from transparent tape imprints (**C**). Stomata viewed under a microscope at 100× magnification. D-Control: diploid control (blue); D-Endo: diploid SEn (orange); T-Control (grey): triploid control; T-Endo: triploid SEn (green).

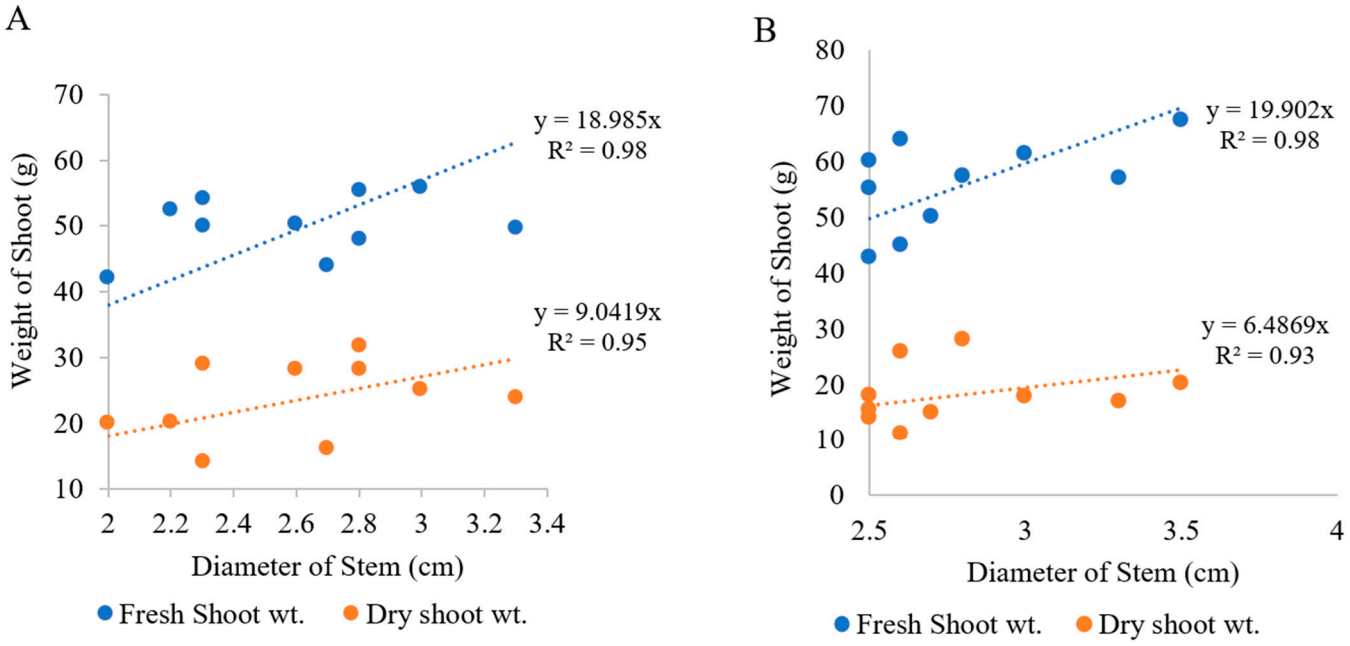


**Figure 16.** Regression analysis of fresh and dry shoot weight in relation to the diameter of the stem in Suver Haze diploid (**A**) and triploid (**B**) plants.

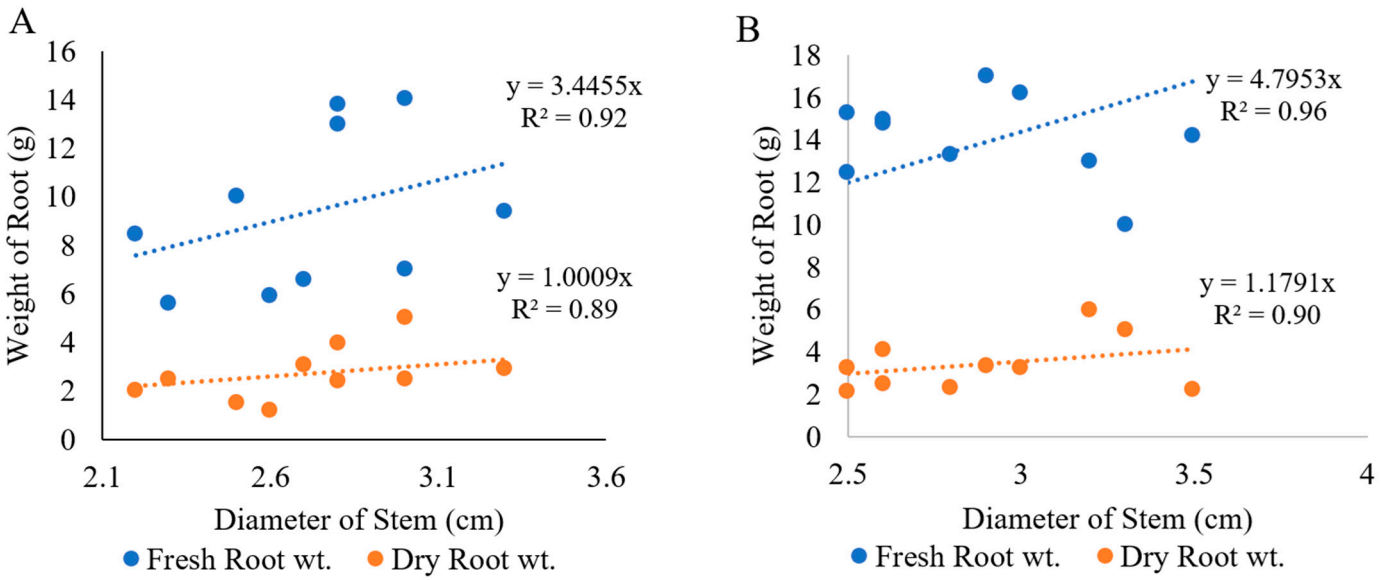


**Figure 17.** Regression analysis of fresh and dry root weight in relation to the diameter of the stem in Suver Haze diploid (**A**) and triploid (**B**) plants.

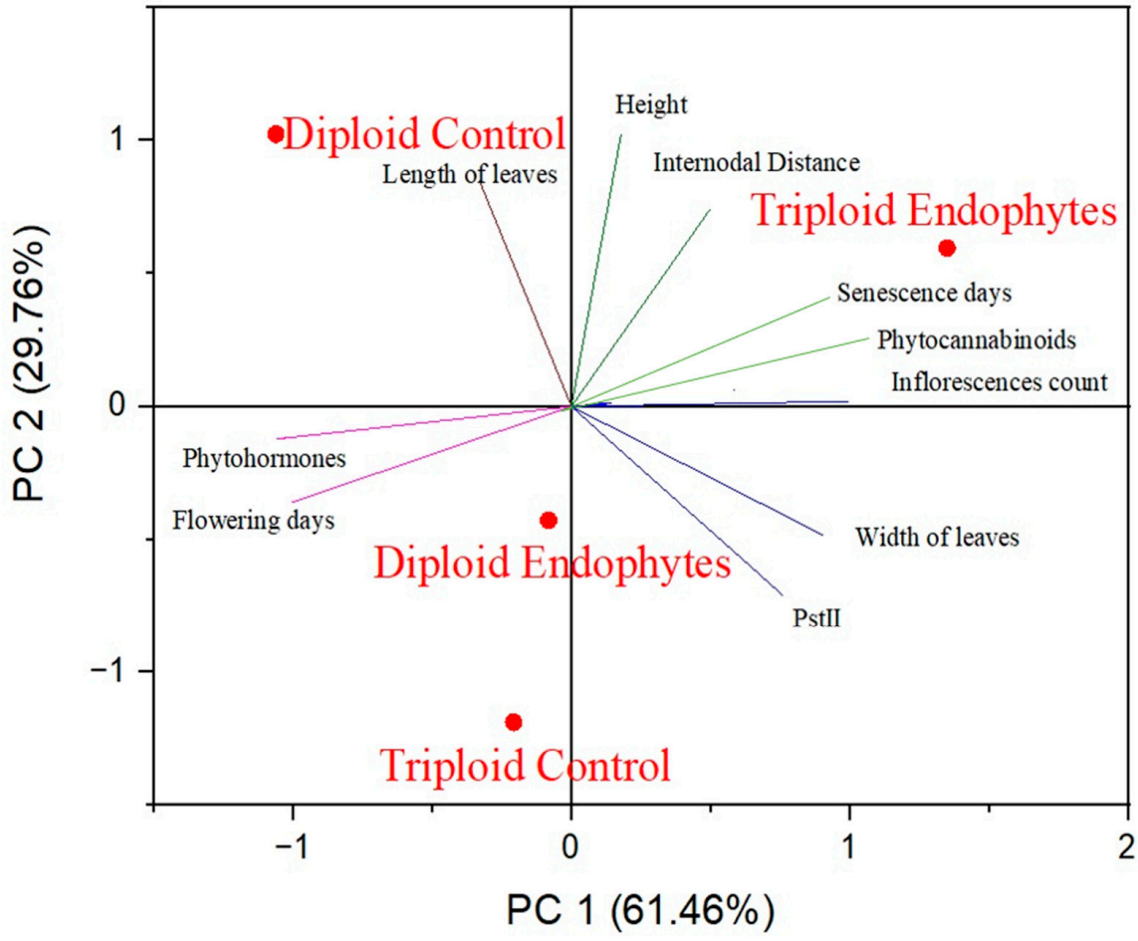


**Figure 18.** Principal component analysis based on the Bray–Curtis dissimilarity between different phenotypic parameters associated with Suver Haze plants grown in a phytotron chamber.

## 4. Discussion

The results of the in vitro study (Exp.1) revealed a high efficacy of cannabis seed endophytes (SEns) in promoting seed germination compared with seed epiphytes (SEps) and the whole seed microbiome (WSM). The promotion potential of SEns was further evaluated *in planta* (Exp.2). SEns reintroduced into the host plant during seed gemmation [11,16] enhanced early plant growth and improved traits in diploid and triploid treated plants compared with untreated plants. Multiple phenotypic improvements included germinant development, vegetative plant growth, and flowering. Microbial diversity in triploid plants was somewhat reduced compared with diploid plants under controlled phytotron conditions. The reduced microbial diversity often occurs in plants exposed to environmental, biotic, and/or abiotic stresses [68], and is hypothesized to assist stressed plants to adapt and thrive [69]. It seems that the lower microbial diversity in Suver Haze triploids may signify differences in the adaptability of different genome sizes. It is interesting that polyploidization in other members of the kingdom of plants also resulted in an increasing reduction in microbiome diversity [16,70]. In this study, we detected a stable *Penicillium* and increased *Chaetomium* and *Bacillus* presence in triploid hemp, possibly responsible for the reduction in phytopathogenic *Fusarium* and *Cladosporium* when compared with diploid host. It is unclear whether improved plant resistance and phenotypic prediction in *Cannabis* polyploids can be predicted by combining plant genetics and microbiome associations, but it will be interesting to evaluate the role of the endophytes in polyploid hemp plants in fields to develop accurate predictions of plant performance under changing environmental conditions.

In terms of phenotypic traits, diploid Suver Haze plants without treatment displayed greater height compared to triploids (weeks 4, 6, 8, 9: $p < 0.05$; weeks 3, 7, 10: $p < 0.01$; week 5: $p < 0.001$), whereas untreated (control) plants were shorter than their endophyte-treated counterparts (weeks 3–10: $p < 0.05$; week 4, 8: $p < 0.01$; week 6: $p < 0.001$). These changes could be also due in part to the genetic differences in the plant that influence their response to treatments [36,71]. This might be driven by differences in cannabis genotype phototropism, the hormonal and growth responses to optimized LED light indoor environments. It has been reported [72–74] that the apical meristem, located at the tips of shoots and roots, is particularly sensitive to light. In the case of shoots, this often leads to upward growth [75–77]. This height disparity is possibly influenced by a complex interplay of Suvar Haze genetics and endophyte interactions, as previously shown in cannabis [78–81]. In this study, triploid plants exhibited an overall greater height than diploids, stating that triploids are made taller than diploids.

According to Fernandes et al., 2023 [82] hemp plant morphology revealed a significant increase in plant height and leaf size with increasing ploidy levels in a cultivar-dependent manner. Based on this study's results, the influence of light on leaf length and width varied between cultivars. Leaves exposed to sufficient light may exhibit increased vigor, cell expansion, and elongation, resulting in longer and wider leaves [83–85]. Although this is a complex biological process, our study demonstrated an important influence of endophytes on this particular trait controlled by various physiological and developmental mechanisms. Controlled lighting conditions created a favorable environment for balanced photosynthetic activity and energy production in plants, which allows to differentiate trade-offs as recognized coexistence mechanisms between mutualistic groups of endophyte and host plants towards enhanced photosynthesis [86]. The variations in leaf length at specific nodes further emphasizes the intricate relationship between endophytes and plant growth. In diploids, untreated plants showed longer leaves at node 2, while seed endophyte-treated diploids displayed extended leaf lengths at nodes 4, 6, and 8. A similar trend was observed in triploids, with treated plants having longer leaves at nodes 2, 6, and 8, except at node 4. It seems this phenomenon could be related to the transition from the vegetative to the flowering stage after 4th node production. This could be also influenced by the microbial dynamics and shifts in communities [87,88] associated with hormonal profile changes over the plant growth stages [89]. Spitzer-Rimon et al., 2022 [90] reported that the hemp

plant shifts into the reproductive stage when a pair of solitary flowers emerges at the 7th node. Examination at the histological level revealed that this transition involves the fresh formation of flower meristems that are absent during the vegetative stage or lying dormant at nodes 4 and 6. Additionally, a significant shift occurs in the transcriptomic profile of genes related to flowering across nodes 4, 6, and 8, as indicated in this study.

We also found that overall cannabis plant biomass formation, dynamics, and productivity can be accurately and rapidly evaluated by the stem diameter assessment. The higher the diameter of the stem, the higher the biomass of the shoots and roots is. It seems that the diameter size is directly proportionate to plant physiological potential for absorbing water and nutrients as well as more physical stability for a higher biomass. This study for the first time reports the direct correlation between the diameter of the stem and aboveground biomass, as well as the diameter of the stem and root biomass for accurate hemp growth prediction [91,92].

Polyploid plants often have larger leaves, which in this study, coincides with a greater number of stomata per photosynthetic surface area for gas exchange, which can increase the uptake of carbon dioxide needed for photosynthesis. However, the naturally smaller leaves of diploid plants underwent greater surface expansion when treated with endophytes compared with triploid plants. It seems that endophytes modify plant leaf characteristics and photosynthetic activities in a host-specific manner. Additionally, the duration of the flowering phase highlighted that endophyte-treated triploids flowered earlier than their untreated counterparts, suggesting that triploid plants remain more physiologically active. The extended days of senescence in both endophyte-treated diploids and triploids indicate that endophyte treatment may prolong plant lifespan in both cultivars by eventually reinforcing the biosynthesis of primary and secondary metabolites, which contribute to the overall health and longevity of the plant [93,94]. The number of axillary branches and inflorescences revealed significant differences. Triploids treated with endophytes had the highest number of axillary branches, while endophyte-treated diploids had the fewest, with untreated cultivars falling in between. Moreover, endophyte-treated plants in both cultivars displayed a higher number of inflorescences, implying the potential for increased phytocannabinoid production. Internodal distances were the longest in seed endophyte-treated triploids and shortest in seed endophyte-treated diploids, with untreated cultivars falling in between. Hence, the results revealed that endophytes could affect the spatial arrangement of nodes with possibly vital consequences to plant physiology and productivity [95,96].

The Fv/Fm values in plants with and without endophytes were within an optimal range for all four cultivars. This study confirms normal growth (i.e., no stress) in both untreated and microbiome-treated plants under optimized (temperature/humidity/light) conditions in the phytotron chambers [97,98]. Further, stomatal imprints revealed a higher stomatal density in triploids compared to diploids. This shift in stomata number should have implications for leaf water use efficiency and gas exchange. The stomata are enabling vital physiological processes and balanced photosynthetic activities [95]. The dynamic change in stem diameter is a good indicator of changes in both the fresh and dry biomass of plants. This funding allows to establish a new, simple, and rapid method to estimate the biomass of the cannabis plant during its developmental growth stages. Principal component analysis showed that the width of the leaves and PstII (photosynthesis) cluster seems to not specifically be associated to any cultivar or treatment tested. Leaf width seems to be an additional important parameter to evaluate the physiological strength of the plant [99–101]. Indeed, leaf width can directly influence photosynthesis, which qualifies this agricultural trait as a good indicator of the efficiency of photosynthesis in symbiotic *Cannabis sativa* L. plants.

## 5. Conclusions

In conclusion, the intricate interplay between ploidy levels, the seed microbiome, and beneficial endophyte treatment influences various aspects of cannabis development and

performance. These findings provide valuable insights into the potential of endophytic symbionts to modulate plant characteristics, flowering times, and overall performance, with implications for the hemp industry and agriculture. PCA analyses demonstrated measurable differentiation between diploid and triploid cannabis hosts and the associated microbiome-induced traits. Further research is needed to unravel the underlying mechanisms behind these study results. The pivotal role of SEns in shaping plant traits in both diploid and triploid hemp lines was observed. To delve deeper into this phenomenon and improve our understanding, comprehensive research that centers on investigating specific parameters, such as the production of secondary metabolites, hormones, and proteins by these plants in interaction with endophytes, under control and field conditions [102–104], should be taken into consideration.

**Author Contributions:** Conceptualization, A.S. and V.V.; methodology, A.S. and V.V.; software, A.S.; validation, A.S., V.V. and T.S.; formal analysis, A.S.; investigation, A.S. and V.V.; resources, V.V.; data curation, A.S. and V.V.; writing—original draft, A.S. and V.V.; writing—review and editing, A.S., V.V. and T.S.; visualization, V.V.; supervision, V.V. and T.S.; project administration, V.V.; funding acquisition, V.V. All authors have read and agreed to the published version of the manuscript.

**Funding:** This research was funded by the National Sciences and Engineering Research Council of Canada (NSERC) Discovery grant (RGPIN-2017-05286) and NSERC Quality Assurance and Quality Control for Cannabis for Production, Products and Training (QAQCC), to V.V.

**Institutional Review Board Statement:** Not applicable.

**Informed Consent Statement:** Not applicable.

**Data Availability Statement:** All data are presented in this paper.

**Acknowledgments:** The authors would like to thank the anonymous reviewers of this paper.

**Conflicts of Interest:** The authors declare no conflicts of interest.

## References

1. Cerino, P.; Buonerba, C.; Cannazza, G.; D'Auria, J.; Ottoni, E.; Fulgione, A.; Di Stasio, A.; Pierri, B.; Gallo, A. A Review of Hemp as Food and Nutritional Supplement. *Cannabis Cannabinoid Res.* **2021**, *6*, 19–27. [CrossRef] [PubMed]
2. Aloo, S.O.; Mwiti, G.; Ngugi, L.W.; Oh, D.-H. Uncovering the secrets of industrial hemp in food and nutrition: The trends, challenges, and new-age perspectives. *Crit. Rev. Food Sci. Nutr.* **2022**, *64*, 5093–5112. [CrossRef] [PubMed]
3. Duque Schumacher, A.G.; Pequito, S.; Pazour, J. Industrial hemp fiber: A sustainable and economical alternative to cotton. *J. Clean. Prod.* **2020**, *268*, 122180. [CrossRef]
4. Vandepitte, K.; Vasile, S.; Vermeire, S.; Vanderhoeven, M.; Van der Borght, W.; Latré, J.; De Raeve, A.; Troch, V. Hemp (*Cannabis sativa* L.) for high-value textile applications: The effective long fiber yield and quality of different hemp varieties, processed using industrial flax equipment. *Ind. Crops Prod.* **2020**, *158*, 112969. [CrossRef]
5. Parvez, A.M.; Lewis, J.D.; Afzal, M.T. Potential of industrial hemp (*Cannabis sativa* L.) for bioenergy production in Canada: Status, challenges and outlook. *Renew. Sustain. Energy Rev.* **2021**, *141*, 110784. [CrossRef]
6. Hilderbrand, R.L. Hemp & Cannabidiol: What is a Medicine? *Mo. Med.* **2018**, *115*, 306–309.
7. Crini, G.; Lichtfouse, E.; Chanet, G.; Morin-Crini, N. Applications of hemp in textiles, paper industry, insulation and building materials, horticulture, animal nutrition, food and beverages, nutraceuticals, cosmetics and hygiene, medicine, agrochemistry, energy production and environment: A review. *Environ. Chem. Lett.* **2020**, *18*, 1451–1476. [CrossRef]
8. Malomo, S.A.; He, R.; Aluko, R.E. Structural and Functional Properties of Hemp Seed Protein Products. *J. Food Sci.* **2014**, *79*, C1512–C1521. [CrossRef]
9. De Prato, L.; Ansari, O.; Hardy, G.E.S.J.; Howieson, J.; O'Hara, G.; Ruthrof, K.X. Morpho-physiology and cannabinoid concentrations of hemp (*Cannabis sativa* L.) are affected by potassium fertilisers and microbes under tropical conditions. *Ind. Crops Prod.* **2022**, *182*, 114907. [CrossRef]
10. Burgel, L.; Hartung, J.; Schibano, D.; Graeff-Hönninger, S. Impact of Different Phytohormones on Morphology, Yield and Cannabinoid Content of *Cannabis sativa* L. *Plants Basel* **2020**, *9*, 725. [CrossRef]
11. Vujanovic, V.; Korber, D.R.; Vujanovic, S.; Vujanovic, J.; Jabaji, S. Scientific Prospects for Cannabis-Microbiome Research to Ensure Quality and Safety of Products. *Microorganisms* **2020**, *8*, 290. [CrossRef] [PubMed]
12. Middleton, H.; Yergeau, É.; Monard, C.; Combier, J.-P.; El Amrani, A. Rhizospheric Plant–Microbe Interactions: miRNAs as a Key Mediator. *Trends Plant Sci.* **2021**, *26*, 132–141. [CrossRef] [PubMed]
13. Azarbad, H.; Tremblay, J.; Bainard, L.D.; Yergeau, E. Relative and Quantitative Rhizosphere Microbiome Profiling Results in Distinct Abundance Patterns. *Front. Microbiol.* **2022**, *12*, 798023. [CrossRef] [PubMed]

14. Cavé-Radet, A.; Correa-Garcia, S.; Monard, C.; El Amrani, A.; Salmon, A.; Ainouche, M.; Yergeau, É. Phenanthrene contamination and ploidy level affect the rhizosphere bacterial communities of *Spartina* spp. *FEMS Microbiol. Ecol.* **2020**, *96*, fiaa156. [CrossRef]
15. Agoussar, A.; Yergeau, E. Engineering the plant microbiota in the context of the theory of ecological communities. *Curr. Opin. Biotechnol.* **2021**, *70*, 220–225. [CrossRef]
16. Vujanovic, V.; Germida, J. Seed endosymbiosis: A vital relationship in providing prenatal care to plants. *Can. J. Plant Sci.* **2017**, *97*, 972–981. [CrossRef]
17. Crawford, S.; Rojas, B.M.; Crawford, E.; Otten, M.; Schoenenberger, T.A.; Garfinkel, A.R.; Chen, H. Characteristics of the Diploid, Triploid, and Tetraploid Versions of a Cannabigerol-Dominant F1 Hybrid Industrial Hemp Cultivar, Cannabis sativa 'Stem Cell CBG'. *Genes* **2021**, *12*, 923. [CrossRef]
18. Parsons, J.L.; Martin, S.L.; James, T.; Golenia, G.; Boudko, E.A.; Hepworth, S.R. Polyploidization for the Genetic Improvement of Cannabis sativa. *Front. Plant Sci.* **2019**, *10*, 476. [CrossRef]
19. Soltis, D.E.; Soltis, P.S. The dynamic nature of polyploid genomes. *Proc. Natl. Acad. Sci. USA* **1995**, *92*, 8089–8091. [CrossRef]
20. Tate, J.A.; Soltis, D.E.; Soltis, P.S. Polyploidy in Plants. In *The Evolution of the Genome*; Elsevier: Amsterdam, The Netherlands, 2005; pp. 371–426. [CrossRef]
21. Bagheri, M.; Mansouri, H. Effect of Induced Polyploidy on Some Biochemical Parameters in *Cannabis sativa* L. *Appl. Biochem. Biotechnol.* **2015**, *175*, 2366–2375. [CrossRef]
22. Chandra, S.; Lata, H.; ElSohly, M.A. (Eds.) *Cannabis sativa L.—Botany and Biotechnology*; Springer: Berlin/Heidelberg, Germany, 2017.
23. Mangena, P. Cell Mutagenic Autopolyploidy Enhances Salinity Stress Toler-Ance in Leguminous Crops. *Cells* **2023**, *12*, 2082. [CrossRef]
24. Islam, M.M.; Deepo, D.M.; Nasif, S.O.; Siddique, A.B.; Hassan, O.; Siddique, A.B.; Paul, N.C. Cytogenetics and Consequences of Polyploidization on Different Biotic-Abiotic Stress Tolerance and the Potential Mechanisms Involved. *Plants* **2022**, *11*, 2684. [CrossRef] [PubMed]
25. Takenaka, S.; Joshi, G.P.; Endo, T.R. Development of self-fertile deletion homozygous and ditelosomic lines for the long arm of chromosome 2A in common wheat. *Genes Genet. Syst.* **2020**, *95*, 95–99. [CrossRef] [PubMed]
26. Madani, H.; Escrich, A.; Hosseini, B.; Sanchez-Muñoz, R.; Khojasteh, A.; Palazon, J. Effect of Polyploidy Induction on Natural Metabolite Production in Medicinal Plants. *Biomolecules* **2021**, *11*, 899. [CrossRef] [PubMed]
27. Weeks, D.P. Gene Editing in Polyploid Crops: Wheat, Camelina, Canola, Potato, Cotton, Peanut, Sugar Cane, and Citrus. In *Progress in Molecular Biology and Translational Science*; Elsevier: Amsterdam, The Netherlands, 2017; Volume 149, pp. 65–80. [CrossRef]
28. Tossi, V.E.; Martínez Tosar, L.J.; Laino, L.E.; Iannicelli, J.; Regalado, J.J.; Escandón, A.S.; Baroli, I.; Causin, H.F.; Pitta-Álvarez, S.I. Impact of polyploidy on plant tolerance to abiotic and biotic stresses. *Front. Plant Sci.* **2022**, *13*, 869423. [CrossRef] [PubMed]
29. Hamarashid, S.H.; Khaledian, Y.; Soleimani, F. In vitro polyploidy-mediated enhancement of secondary metabolites content in *Stachys byzantina* L. *Genet. Resour. Crop Evol.* **2022**, *69*, 719–728. [CrossRef]
30. Zheng, M.; Li, J.; Zeng, C.; Liu, X.; Chu, W.; Lin, J.; Wang, F.; Wang, W.; Guo, W.; Xin, M.; et al. Subgenome-biased expression and functional diversification of a $Na^+/H^+$ antiporter homoeologs in salt tolerance of polyploid wheat. *Front. Plant Sci.* **2022**, *13*, 1072009. [CrossRef]
31. Roy, S.; Mathur, P.; Chakraborty, A.P.; Saha, S.P. (Eds.) *Plant Stress: Challenges and Management in the New Decade*; Advances in Science, Technology & Innovation; Springer International Publishing: Cham, Switzerland, 2022. [CrossRef]
32. Powell, A.J.; Kim, S.H.; Cordero, J.; Vujanovic, V. Protocooperative Effect of *Sphaerodes mycoparasitica* Biocontrol and Crop Genotypes on FHB Mycotoxin Reduction in Bread and Durum Wheat Grains Intended for Human and Animal Consumption. *Microorganisms* **2023**, *11*, 159. [CrossRef]
33. Powell, A.J.; Vujanovic, V. Evolution of Fusarium Head Blight Management in Wheat: Scientific Perspectives on Biological Control Agents and Crop Genotypes Protocooperation. *Appl. Sci.* **2021**, *11*, 8960. [CrossRef]
34. Miller, G. Industrial Hemp Root Length Density and Distribution under Polyethylene Mulch with Drip Irrigation. *HortScience* **2022**, *57*, 1356–1362. [CrossRef]
35. Park, J.; Collado, C.E.; Lam, V.P.; Hernández, R. Flowering Response of *Cannabis sativa* L. 'Suver Haze' under Varying Daylength-Extension Light Intensities and Durations. *Horticulturae* **2023**, *9*, 526. [CrossRef]
36. Stegmeier, R.J. Statistical Analyses of Hemp Cannabinoid Test Results. In *Senior Honors Projects, 2020-Current*; James Madison University Publisher: Harrisonburg, VA, USA, 2022; Volume 136, pp. 1–56. Available online: https://commons.lib.jmu.edu/honors202029/136 (accessed on 1 April 2024).
37. Mendel, P.; Lalge, A.B.; Vyhnanek, T.; Kalousek, P.; Maassen, H.; Havel, L. Progress in Early Sex Determination of Cannabis Plant by DNA Markers. *MendelNet* **2016**, *23*, 731–735. Available online: https://www.researchgate.net/publication/309772639 (accessed on 1 April 2024).
38. Törjek, O.; Bucherna, N.; Kiss, E.; Homoki, H.; Finta-Korpelova, Z.; Bocsa, I.; Nagy, I.; Heszky, L.E. Novel male-specific molecular markers (MADC5, MADC6) in hemp. *Euphytica* **2002**, *127*, 209–218. [CrossRef]
39. Barcaccia, G.; Palumbo, F.; Scariolo, F.; Vannozzi, A.; Borin, M.; Bona, S. Potentials and Challenges of Genomics for Breeding Cannabis Cultivars. *Front. Plant Sci.* **2020**, *11*, 573299. [CrossRef]

40. Tamura, K.; Nei, M. Estimation of the number of nucleotide substitutions in the control region of mitochondrial DNA in humans and chimpanzees. *Mol. Biol. Evol.* **1993**, *10*, 512–526. [CrossRef]
41. Tamura, K.; Stecher, G.; Kumar, S. MEGA11: Molecular Evolutionary Genetics Analysis Version 11. *Mol. Biol. Evol.* **2021**, *38*, 3022–3027. [CrossRef]
42. Suriyong, S.; Krittigamas, N.; Pinmanee, S.; Punyalue, A.; Vearasilp, S. Influence of Storage Conditions on Change of Hemp Seed Quality. *Agric. Agric. Sci. Procedia* **2015**, *5*, 170–176. [CrossRef]
43. Dumigan, C.R.; Deyholos, M.K. Cannabis Seedlings Inherit Seed-Borne Bioactive and Anti-Fungal Endophytic Bacilli. *Plants* **2022**, *11*, 2127. [CrossRef]
44. Punja, Z.K.; Collyer, D.; Scott, C.; Lung, S.; Holmes, J.; Sutton, D. Pathogens and Molds Affecting Production and Quality of *Cannabis sativa* L. *Front. Plant Sci.* **2019**, *10*, 1120. [CrossRef]
45. Hubbard, M.; Germida, J.; Vujanovic, V. Fungal endophytes improve wheat seed germination under heat and drought stress. *Botany* **2012**, *90*, 137–149. [CrossRef]
46. Moroenyane, I.; Tremblay, J.; Yergeau, É. Soybean Microbiome Recovery After Disruption is Modulated by the Seed and Not the Soil Microbiome. *Phytobiomes J.* **2021**, *5*, 418–431. [CrossRef]
47. Kumari, V.; Vujanovic, V. Transgenerational benefits of endophytes on resilience and antioxidant genes expressions in pea (*Pisum sativum* L.) under osmotic stress. *Acta Physiol. Plant.* **2020**, *42*, 49. [CrossRef]
48. Petit, J.; Salentijn, E.M.J.; Paulo, M.-J.; Denneboom, C.; Trindade, L.M. Genetic Architecture of Flowering Time and Sex Determination in Hemp (*Cannabis sativa* L.): A Genome-Wide Association Study. *Front. Plant Sci.* **2020**, *11*, 569958. [CrossRef]
49. Wei, G.; Ning, K.; Zhang, G.; Yu, H.; Yang, S.; Dai, F.; Dong, L.; Chen, S. Compartment Niche Shapes the Assembly and Network of Cannabis sativa-Associated Microbiome. *Front. Microbiol.* **2021**, *12*, 714993. [CrossRef] [PubMed]
50. Tao, J.; Xiang, J.; Jiang, M.; Kuang, S.; Peng, X.; Li, H. A Microtitre Plate Dilution Method for Minimum Killing Concentration Is Developed to Evaluate Metabolites-Enabled Killing of Bacteria by β-lactam Antibiotics. *Front. Mol. Biosci.* **2022**, *9*, 878651. [CrossRef]
51. Pal, G.; Kumar, K.; Verma, A.; Verma, S.K. Seed inhabiting bacterial endophytes of maize promote seedling establishment and provide protection against fungal disease. *Microbiol. Res.* **2022**, *255*, 126926. [CrossRef]
52. Punja, Z.K.; Holmes, J.E. Hermaphroditism in Marijuana (*Cannabis sativa* L.) Inflorescences—Impact on Floral Morphology, Seed Formation, Progeny Sex Ratios, and Genetic Variation. *Front. Plant Sci.* **2020**, *11*, 718. [CrossRef]
53. Raj, R.; Walker, J.P.; Pingale, R.; Nandan, R.; Naik, B.; Jagarlapudi, A. Leaf area index estimation using top-of-canopy airborne RGB images. *Int. J. Appl. Earth Obs. Geoinf.* **2021**, *96*, 102282. [CrossRef]
54. Schrader, J.; Shi, P.; Royer, D.L.; Peppe, D.J.; Gallagher, R.V.; Li, Y.; Wang, R.; Wright, I.J. Leaf size estimation based on leaf length, width and shape. *Ann. Bot.* **2021**, *128*, 395–406. [CrossRef]
55. Kim, S.H.; Lahlali, R.; Karunakaran, C.; Vujanovic, V. Specific Mycoparasite-Fusarium Graminearum Molecular Signatures in Germinating Seeds Disabled Fusarium Head Blight Pathogen's Infection. *Int. J. Mol. Sci.* **2021**, *22*, 2461. [CrossRef]
56. Tang, K.; Struik, P.C.; Amaducci, S.; Stomph, T.-J.; Yin, X. Hemp (*Cannabis sativa* L.) leaf photosynthesis in relation to nitrogen content and temperature: Implications for hemp as a bio-economically sustainable crop. *GCB Bioenergy* **2017**, *9*, 1573–1587. [CrossRef]
57. Gao, K.; Hutchins, D.A.; Beardall, J. (Eds.) *Research Methods of Environmental Physiology in Aquatic Sciences*; Springer: Singapore, 2021. [CrossRef]
58. Banks, J.M. Chlorophyll fluorescence as a tool to identify drought stress in Acer genotypes. *Environ. Exp. Bot.* **2018**, *155*, 118–127. [CrossRef]
59. Hubbard, M.; Germida, J.J.; Vujanovic, V. Fungal endophytes enhance wheat heat and drought tolerance in terms of grain yield and second-generation seed viability. *J. Appl. Microbiol.* **2014**, *116*, 109–122. [CrossRef]
60. Schletz, R. Stomata Densities of Developing and Mature Leaves of Geraniums. *ESSAI* **2008**, *6*, 142. Available online: https://dc.cod.edu/cgi/viewcontent.cgi?referer=&httpsredir=1&article=1084&context=essai (accessed on 1 April 2024).
61. Haworth, M.; Marino, G.; Materassi, A.; Raschi, A.; Scutt, C.P.; Centritto, M. The functional significance of the stomatal size to density relationship: Interaction with atmospheric [$CO_2$] and role in plant physiological behaviour. *Sci. Total Environ.* **2023**, *863*, 160908. [CrossRef]
62. Millstead, L.; Jayakody, H.; Patel, H.; Kaura, V.; Petrie, P.R.; Tomasetig, F.; Whitty, M. Accelerating Automated Stomata Analysis Through Simplified Sample Collection and Imaging Techniques. *Front. Plant Sci.* **2020**, *11*, 580389. [CrossRef] [PubMed]
63. Ivosev, G.; Burton, L.; Bonner, R. Dimensionality Reduction and Visualization in Principal Component Analysis. *Anal. Chem.* **2008**, *80*, 4933–4944. [CrossRef]
64. Mishra, S.; Sarkar, U.; Taraphder, S.; Datta, S.; Swain, D.; Saikhom, R.; Panda, S.; Laishram, M. Principal Component Analysis. *Int. J. Livest. Res.* **2017**, *1*, 100. [CrossRef]
65. Abdullah, M.; Khairurrijal, K. A Simple Method for Determining Surface Porosity Based on SEM Images Using OriginPro Software. *Indones. J. Phys.* **2016**, *20*, 37–40. [CrossRef]
66. Cao, X.H.; Stojkovic, I.; Obradovic, Z. A robust data scaling algorithm to improve classification accuracies in biomedical data. *BMC Bioinform.* **2016**, *17*, 359. [CrossRef]
67. Seleþchi, E.D.; Duliu, O.G. Image processing and data analysis in computed tomography. *Rom. J. Phys.* **2007**, *52*, 667–675. Available online: https://rjp.nipne.ro/2007_52_5-6/0667_0677.pdf (accessed on 1 April 2024).

68. Vujanovic, V.; Brisson, J. A comparative study of endophytic mycobiota in leaves of Acer saccharum in eastern North America. *Mycol. Prog.* **2002**, *1*, 147–154. [CrossRef]
69. Vujanovic, V.; Islam, M.N.; Daida, P. Transgenerational role of seed mycobiome—An endosymbiotic fungal composition as a prerequisite to stress resilience and adaptive phenotypes in Triticum. *Sci. Rep.* **2019**, *9*, 18483. [CrossRef] [PubMed]
70. Gruet, C.; Muller, D.; Moënne-Loccoz, Y. Significance of the Diversification of Wheat Species for the Assembly and Functioning of the Root-Associated Microbiome. *Front. Microbiol.* **2022**, *12*, 782135. [CrossRef] [PubMed]
71. Darby, D.H.; Bruce, J.; Krezinski, I.; Ruhl, L. 2020 Hemp Flower Variety Trial. *UVM Northwest Crops Soils Program* **2021**, *435*, 18. Available online: https://scholarworks.uvm.edu/nwcsp/435/ (accessed on 1 April 2024).
72. Benková, E.; Hejátko, J. Hormone interactions at the root apical meristem. *Plant Mol. Biol.* **2009**, *69*, 383–396. [CrossRef] [PubMed]
73. Kerstetter, R.A.; Hake, S. Shoot Meristem Formation in Vegetative Development. *Plant Cell* **1997**, 1001–1010. [CrossRef]
74. Pfeiffer, A.; Janocha, D.; Dong, Y.; Medzihradszky, A.; Schöne, S.; Daum, G.; Suzaki, T.; Forner, J.; Langenecker, T.; Rempel, E.; et al. Integration of light and metabolic signals for stem cell activation at the shoot apical meristem. *eLife* **2016**, *5*, e17023. [CrossRef]
75. Lund, J.B.; Blom, T.J.; Aaslyng, J.M. End-of-day Lighting with Different Red/Far-red Ratios Using Light-emitting Diodes Affects Plant Growth of Chrysanthemum × morifolium Ramat. 'Coral Charm'. *HortScience* **2007**, *42*, 1609–1611. [CrossRef]
76. Munir, M.; Alhajhoj, M.R. Plant height control of obligate long day herbaceous annuals using plant growth retardants and light. *J. Appl. Hortic.* **2017**, *19*, 241–244. [CrossRef]
77. Ying, Q.; Kong, Y.; Zheng, Y. Growth and Appearance Quality of Four Microgreen Species under Light-emitting Diode Lights with Different Spectral Combinations. *HortScience* **2020**, *55*, 1399–1405. [CrossRef]
78. Mattoo, A.J.; Nonzom, S. Endophytic fungi: Understanding complex cross-talks. *Symbiosis* **2021**, *83*, 237–264. [CrossRef]
79. Mushtaq, S.; Shafiq, M.; Tariq, M.R.; Sami, A.; Nawaz-ul-Rehman, M.S.; Bhatti, M.H.T.; Haider, M.S.; Sadiq, S.; Abbas, M.T.; Hussain, M.; et al. Interaction between bacterial endophytes and host plants. *Front. Plant Sci.* **2023**, *13*, 1092105. [CrossRef] [PubMed]
80. Pathak, P.; Rai, V.K.; Can, H.; Singh, S.K.; Kumar, D.; Bhardwaj, N.; Roychowdhury, R.; De Azevedo, L.C.B.; Kaushalendra; Verma, H.; et al. Plant-Endophyte Interaction during Biotic Stress Management. *Plants* **2022**, *11*, 2203. [CrossRef] [PubMed]
81. Rani, S.; Kumar, P.; Dahiya, P.; Maheshwari, R.; Dang, A.S.; Suneja, P. Endophytism: A Multidimensional Approach to Plant–Prokaryotic Microbe Interaction. *Front. Microbiol.* **2022**, *13*, 861235. [CrossRef]
82. Fernandes, H.P.; Choi, Y.H.; Vrieling, K.; De Bresser, M.; Sewalt, B.; Tonolo, F. Cultivar-dependent phenotypic and chemotypic responses of drug-type *Cannabis sativa* L. to polyploidization. *Front. Plant Sci.* **2023**, *14*, 1233191. [CrossRef]
83. Falster, D.S.; Westoby, M. Leaf size and angle vary widely across species: What consequences for light interception? *New Phytol.* **2003**, *158*, 509–525. [CrossRef]
84. Humphries, E.C.; Wheeler, A.W. The Physiology of Leaf Growth. *Annu. Rev. Plant Physiol.* **1963**, *14*, 385–410. [CrossRef]
85. Saebo, A.; Krekling, T.; Appelgren, M. Light quality affects photosynthesis and leaf anatomy of birch plantlets in vitro. *Plant Cell Tissue Organ Cult.* **1995**, *41*, 177–185. [CrossRef]
86. Santangelo, J.S.; Kotanen, P.M. Nonsystemic fungal endophytes increase survival but reduce tolerance to simulated herbivory in subarctic *Festuca rubra*. *Ecosphere* **2016**, *7*, e01260. [CrossRef]
87. Chaparro, J.M.; Badri, D.V.; Vivanco, J.M. Rhizosphere microbiome assemblage is affected by plant development. *ISME J.* **2014**, *8*, 790–803. [CrossRef] [PubMed]
88. Hesami, M.; Pepe, M.; Jones, A.M.P. Morphological Characterization of *Cannabis sativa* L. Throughout Its Complete Life Cycle. *Plants* **2023**, *12*, 3646. [CrossRef] [PubMed]
89. Backer, R.; Schwinghamer, T.; Rosenbaum, P.; McCarty, V.; Eichhorn Bilodeau, S.; Lyu, D.; Ahmed, M.B.; Robinson, G.; Lefsrud, M.; Wilkins, O.; et al. Closing the Yield Gap for Cannabis: A Meta-Analysis of Factors Determining Cannabis Yield. *Front. Plant Sci.* **2019**, *10*, 495. [CrossRef]
90. Spitzer-Rimon, B.; Shafran-Tomer, H.; Gottlieb, G.H.; Doron-Faigenboim, A.; Zemach, H.; Kamenetsky-Goldstein, R.; Flaishman, M. Non-photoperiodic transition of female cannabis seedlings from juvenile to adult reproductive stage. *Plant Reprod.* **2022**, *35*, 265–277. [CrossRef]
91. Bektas, H.; Hohn, C.E.; Lukaszewski, A.J.; Waines, J.G. On the Possible Trade-Off between Shoot and Root Biomass in Wheat. *Plants* **2023**, *12*, 2513. [CrossRef]
92. Gichangi, E.M.; Njarui, D.M.G.; Gatheru, M.J. Plant shoots and roots biomass of brachiaria grasses and their effects on soil carbon in the semi-arid tropics of Kenya. *Trop. Subtrop. Agroecosystems* **2017**, *20*, 65–74. [CrossRef]
93. Ali, S.; Charles, T.C.; Glick, B.R. Delay of flower senescence by bacterial endophytes expressing 1-aminocyclopropane-1-carboxylate deaminase. *J. Appl. Microbiol.* **2012**, *113*, 1139–1144. [CrossRef]
94. Zhang, H.; Li, X.; White, J.F.; Wei, X.; He, Y.; Li, C. Epichloë Endophyte Improves Ergot Disease Resistance of Host (*Achnatherum inebrians*) by Regulating Leaf Senescence and Photosynthetic Capacity. *J. Plant Growth Regul.* **2022**, *41*, 808–817. [CrossRef]
95. Naveed, M.; Mitter, B.; Reichenauer, T.G.; Wieczorek, K.; Sessitsch, A. Increased drought stress resilience of maize through endophytic colonization by *Burkholderia phytofirmans* PsJN and Enterobacter sp. FD17. *Environ. Exp. Bot.* **2014**, *97*, 30–39. [CrossRef]
96. Purushotham, N.; Jones, E.; Monk, J.; Ridgway, H. Community Structure of Endophytic Actinobacteria in a New Zealand Native Medicinal Plant *Pseudowintera colorata* (Horopito) and Their Influence on Plant Growth. *Microb. Ecol.* **2018**, *76*, 729–740. [CrossRef]

97. Chitarra, W.; Siciliano, I.; Ferrocino, I.; Gullino, M.L.; Garibaldi, A. Effect of Elevated Atmospheric $CO_2$ and Temperature on the Disease Severity of Rocket Plants Caused by Fusarium Wilt under Phytotron Conditions. *PLoS ONE* **2015**, *10*, e0140769. [CrossRef] [PubMed]
98. Poudyal, D.; Rosenqvist, E.; Ottosen, C.-O. Phenotyping from lab to field—Tomato lines screened for heat stress using Fv/Fm maintain high fruit yield during thermal stress in the field. *Funct. Plant Biol.* **2019**, *46*, 44. [CrossRef] [PubMed]
99. Cano, F.J.; Sharwood, R.E.; Cousins, A.B.; Ghannoum, O. The role of leaf width and conductances to $CO_2$ in determining water use efficiency in C4 grasses. *New Phytol.* **2019**, *223*, 1280–1295. [CrossRef] [PubMed]
100. Reich, P.B.; Ellsworth, D.S.; Walters, M.B. Leaf structure (specific leaf area) modulates photosynthesis–nitrogen relations: Evidence from within and across species and functional groups. *Funct. Ecol.* **1998**, *12*, 948–958. [CrossRef]
101. Ackerly, D.D.; Reich, P.B. Convergence and correlations among leaf size and function in seed plants: A comparative test using independent contrasts. *Am. J. Bot.* **1999**, *86*, 1272–1281. [CrossRef]
102. Kumari, P.; Deepa, N.; Trivedi, P.K.; Singh, B.K.; Srivastava, V.; Singh, A. Plants and endophytes interaction: A "secret wedlock" for sustainable biosynthesis of pharmaceutically important secondary metabolites. *Microb. Cell Factories* **2023**, *22*, 226. [CrossRef]
103. Seema, N.; Hamayun, M.; Hussain, A.; Shah, M.; Irshad, M.; Qadir, M.; Iqbal, A.; Alrefaei, A.F.; Ali, S. Endophytic *Fusarium proliferatum* Reprogrammed Phytohormone Production and Antioxidant System of Oryza sativa under Drought Stress. *Agronomy* **2023**, *13*, 873. [CrossRef]
104. Ali, R.; Gul, H.; Hamayun, M.; Rauf, M.; Iqbal, A.; Hussain, A.; Lee, I.-J. Endophytic Fungi Controls the Physicochemical Status of Maize Crop under Salt Stress. *Pol. J. Environ. Stud. Vol.* **2022**, *31*, 561–573. [CrossRef]